Characteristics of a Dual-Slotted Circulation Control Wing of Low Aspect Ratio Intended for Naval Hydrodynamic Applications

Ernest O. Rogers[*], Martin J. Donnelly[**]

Hydromechanics Directorate
Naval Surface Warfare Center, Carderock Division
West Bethesda, MD 20817

ABSTRACT

An experimental investigation was conducted in a water tunnel to explore the application of Coanda-effect circulation control to low aspect ratio wings. The facility was the Large Cavitation Channel in Memphis, TN. The intended application is to high-lift control-surfaces (appendages) on underwater naval vehicles. Test results are interpreted in light of both theory and the extensive experience with circulation control (CC) technology at NSWCCD. The semi-span wing test model with a taper ratio of 0.76 was mounted on a load cell; a reflection plane provided for an effective aspect ratio of 2. Dual upper/lower trailing edge tangential jet slots were incorporated for bi-directional force generation. Findings include: finite-span effects on CC augmented lift are consistent with the effects on conven-tional lift-due-to-angle-of-attack, and cavitation in the Coanda wall jet region does not result in jet detachment or an abrupt lift stall. Wing lift augmentation ratios are up to 36 and meet expectations. Unexpected virtues of a dual-slotted configuration were found that enhance the value of CC to ship and VSTOL aircraft applications. A small flow from the second slot will significantly extend the lift capability beyond that of single slot operation by preventing what is believed to be the adverse effects of excessive turning of the wall jet at high momentum coefficients. Dual slot flow produces a merger of the two wall jets into a free planar jet that enables static thrust vectoring of the jet momentum flux over the full 0-360 deg range. This steerable-jet provides a jet-flap mode of lift development for use at very low vehicle speeds, as an extension of the high efficiency CC mode.

[*] Aerospace Engineer, Marine and Aviation Dept.
[**] Mechanical Engineer, Propulsion and Fluid Systems Dept.

OBJECTIVES

For hydrodynamic applications of circulation control (CC), there existed certain technical questions that had not been addressed in previous evaluations of this form of active flow control for high lift. The unknowns included: (1) ability to predict the performance of a low aspect ratio CC planform, (2) cavitation properties of the trailing edge Coanda wall jet, (3) attributes of dual slots, including wake-filling. The answers to these questions, among others, were the objectives of an investigation in a water tunnel of a CC hydrofoil (wing) of effective aspect ratio 2, Figure 1.

Figure 1(a). CC high-lift control surface (wing) of aspect ratio 2 in the LCC 10-ft x 10-ft water tunnel. Slot flow checkout in air.
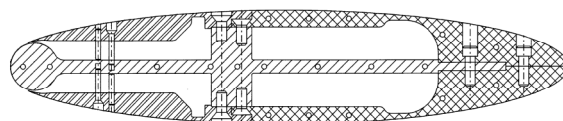

Figure 1(b). Model cross section.

e

1. REPORT DATE **JAN 2004**	2. REPORT TYPE	3. DATES COVERED **-**

4. TITLE AND SUBTITLE	5a. CONTRACT NUMBER
Characteristics of a Dual-Slotted Circulation Control Wing of Low Aspect Ratio Intended for Naval Hydrodynamic Applications	5b. GRANT NUMBER
	5c. PROGRAM ELEMENT NUMBER
6. AUTHOR(S)	5d. PROJECT NUMBER
	5e. TASK NUMBER
	5f. WORK UNIT NUMBER

7. PERFORMING ORGANIZATION NAME(S) AND ADDRESS(ES) **Naval Surface Warfare Center,Carderock Division,Hydromechanics Directorate,West Bethesda,MD,20817**	8. PERFORMING ORGANIZATION REPORT NUMBER
9. SPONSORING/MONITORING AGENCY NAME(S) AND ADDRESS(ES)	10. SPONSOR/MONITOR'S ACRONYM(S)
	11. SPONSOR/MONITOR'S REPORT NUMBER(S)

12. DISTRIBUTION/AVAILABILITY STATEMENT
Approved for public release; distribution unlimited

13. SUPPLEMENTARY NOTES
The original document contains color images.

14. ABSTRACT

An experimental investigation was conducted in a water tunnel to explore the application of Coanda-effect circulation control to low aspect ratio wings. The facility was the Large Cavitation Channel in Memphis, TN. The intended application is to high-lift controlsurfaces (appendages) on underwater naval vehicles. Test results are interpreted in light of both theory and the extensive experience with circulation control (CC) technology at NSWCCD. The semi-span wing test model with a taper ratio of 0.76 was mounted on a load cell; a reflection plane provided for an effective aspect ratio of 2. Dual upper/lower trailing edge tangential jet slots were incorporated for bi-directional force generation. Findings include: finite-span effects on CC augmented lift are consistent with the effects on conventional lift-due-to-angle-of-attack, and cavitation in the Coanda wall jet region does not result in jet detachment or an abrupt lift stall. Wing lift augmentation ratios are up to 36 and meet expectations. Unexpected virtues of a dual-slotted configuration were found that enhance the value of CC to ship and VSTOL aircraft applications. A small flow from the second slot will significantly extend the lift capability beyond that of single slot operation by preventing what is believed to be the adverse effects of excessive turning of the wall jet at high momentum coefficients. Dual slot flow produces a merger of the two wall jets into a free planar jet that enables static thrust vectoring of the jet momentum flux over the full 0-360 deg range. This steerable-jet provides a jet-flap mode of lift development for use at very low vehicle speeds, as an extension of the high efficiency CC mode.

15. SUBJECT TERMS					

16. SECURITY CLASSIFICATION OF:			17. LIMITATION OF ABSTRACT	18. NUMBER OF PAGES **29**	19a. NAME OF RESPONSIBLE PERSON
a. REPORT **unclassified**	b. ABSTRACT **unclassified**	c. THIS PAGE **unclassified**			

NOMENCLATURE

AC	aerodynamic center
AOA	angle-of-attack
AR	aspect ratio, $2s/c$
c	chord
C_D	drag coefficient (D/qS)
C_{Di}	Induced drag coefficient
C_ℓ	airfoil lift coefficient
C_L	lift coefficient (L/qS)
$C_{L\Gamma}$	circulatory component of C_L
C_m	pitching moment coefficient (M/qSc)
C_p	pressure coefficient ($(P_{local}-P_\infty)/q$)
C_μ	slot momentum coef. ($\dot{m}V_{jet}/qS$)
e	Oswald span lifting efficiency factor
h	slot height (gap)
hp	horsepower for slot flow
$\dot{m}$	slot mass flow rate
P_d	duct pressure
P_{local}	surface pressure
P_∞	freestream static pressure
q	dynamic pressure ($1/2\,\rho\,V_\infty^2$)
r	radius of curvature
s	span (24 inches), root to tip
S	planform area
V_∞	freestream velocity
V_{jet}	slot exit velocity, calculated
α_i	induced angle of attack
α_e	effective AOA
α_{geo}	geometric AOA (pitch)
ρ	density
σ	cavitation number

TECHNOLOGY BACKGROUND

The force that results from flow past a surface is strongly influenced by the boundary condition at the downstream edge. This boundary condition is the location where the wake departs the surface--equivalent to the rear stagnation point in conventional airfoil theory--and is determined by where the upper and lower surface flows separate at or near the trailing edge. Any physical means of influencing the location of the flow separation points will correspondingly change the net fluid forces developed on the surface.

The present concept considers a non-mechanical method of influencing the trailing edge boundary condition, Figure 2, with the demonstrated potential to achieve force production beyond that available conventionally. This technique, known as circulation control (CC), is based on the ability of a wall jet emitted from a tangential slot to remain attached to a curved surface, the Coanda effect.[1,2] The surface flow upstream of the blowing slot is entrained into the emerging jet. Through an exchange of momentum, the wall jet, which is directed over the rounded trailing edge of a planar surface, changes the relative momentum levels of upper/lower surface flows, thereby shifting the location of the flow merger and hence the wake formation point. The absence of a sharp trailing edge removes the constraint of an enforced Kutta condition, allowing the circulation of the wing to be freely influenced by active flow control. Effectively, the rear stagnation point is moved, as depicted in Figure 2, with the leading edge stagnation point moving in concert in accordance with basic airfoil theory. Large increases in lift coefficient result, well beyond that available from conventional airfoils. Even in the absence of a sharp
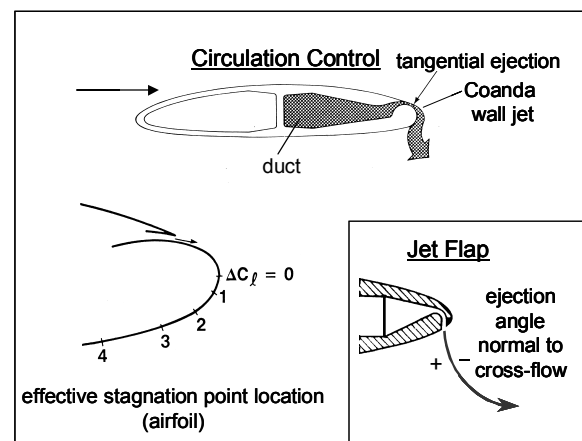

Figure 2. Circulation control airfoil configuration: rounded trailing edge with tangential mass ejection; a jet-flap configuration is shown for comparison. A change in effective stagnation point location increments lift as indicated.

trailing edge, lift response to pitch angle, with or without blowing, is essentially the same as for conventional lifting surfaces.

The lift augmentation approach described above involves jet efflux emitted *tangent* to the airfoil, with the intention that it remain attached for some distance, as is the nature of the Coanda effect. The inverse of this is the jet-flap, a well known lift augmentation technique that depends on mass ejection from the trailing edge in a direction approximately *perpendicular* to the airfoil surface so as to form a cross-flow jet with respect to the local flow. The pressure differential developed in the downstream flow field across this necessarily curved free momentum sheet transfers back onto the airfoil surface and produces essentially the same chordwise load distribution as arises from the Coanda tangential jet approach. The practical difference is that the jet-flap is an inefficient technique, taking many times more slot pumping power than the CC tangential ejection

approach. One favorable attribute is that the jet-flap can convert extreme values of jet momentum coefficients into lift increments, although in the limit it just incrementally produces a jet reaction force (non-circulatory lift). The jet-flap was not to be a focus of the current investigation because of the much higher efficiency achieved by using a tangential jet. There is, however, something of a jet-flap element to the CC function when the jet has excess momentum as it departs the trailing edge region. Furthermore, the findings from the current investigation have refocused interest in the inter-relationship of these two forms of lift enhancement.

Performance of a CC device is characterized as a function of the slot flow momentum coefficient, $C\mu$, which is the ratio of jet momentum flux to free stream dynamic pressure and surface area. For incompressible flow with a full span slot of constant gap h/c:

$$C\mu = \dot{m}\,V_{jet}\,/\,(qS), \qquad (1)$$
$$= 2\,(h/c)\,(V_{jet}\,/\,V_\infty)^2,$$
$$= 2\,(h/c)\,(Pd/q),$$
$$= (550\,hp/S)^{2/3}\,(2h/c)^{1/3}\,(4/\rho)^{2/3}\,/\,V_\infty^2.$$

There is no limit to the attainable value of $C\mu$ since it increases as speed declines, for a given slot pumping power, hp. The usual range of $C\mu$ can be envisioned as from 0.0 to about 0.2; above 0.3, excess momentum in the wake can become problematic, unless the trailing edge is of a design to limit jet turning angle. A gain, or augmentation ratio, is defined as the ratio of the incremental lift force developed to the increment in jet momentum. Augmentation ratios of up to 80 have been found for CC airfoils (wings of infinite aspect ratio) when operating at low values of $C\mu$ (<0.02) where the response to blowing is linear. For a wing, the augmentation ratio would be lower, due to vortex induced downwash effects. At higher levels of $C\mu$, the lift increment becomes proportional to the square-root of $C\mu$. As implied by the square-root relationship and with the subtraction of the presumed jet reaction force, circulatory lift from any form of circulation control seems to asymptote to a limit. In addition to this upper bound of circulatory gain, there is the potential for the usual limits due to leading edge separation, Mach number effects, cavitation, or excessive turning of the Coanda wall jet. And there may be limits imposed by the test facility size: model chord to tunnel height, excessive wake blockage, jet impingement on the floor, and side-wall boundary layer separation due to imposition of the pressure field from the high-lift surface.

Potential Applications

There have been a number of proof-of-concepts of CC as applied to moderate to high aspect ratio wings and blades for aviation application.[3,4] Currently, there is an interest in underwater applications of this technology, which would involve lifting surfaces of low aspect ratio (AR); AR=2 is typical. The interest in naval applications is prompted by both the expected ability to develop at least twice as much force as a conventional appendage (control surface), and for some applications, the possible option of converting a moveable surface into one that is fixed. In addition, there is the inherent feature of CC where for a given slot flow rate the momentum coefficient increases and hence the lift coefficient is higher as free stream speed *declines*. These characteristics are attractive for enhancing vehicle maneuverability at low speed. CC could be applied to such appendages as rudders, bowplanes, sternplanes, anti-roll fins, or even to sails (bridge fairwater). For those applications, there would be dual (symmetrical) trailing edge slots for bi-directional force generation.

THEORETICAL CONSIDERATIONS

Airfoil (2D) and Wing (3D) Lift Augmentation

Figure 3 illustrates how well the calculated potential (inviscid) flow pressure distribution for a specified lift and angle of attack (AOA) generally matches the experimental measurements on a CC airfoil. For the airfoil case of an infinite wing, the loading
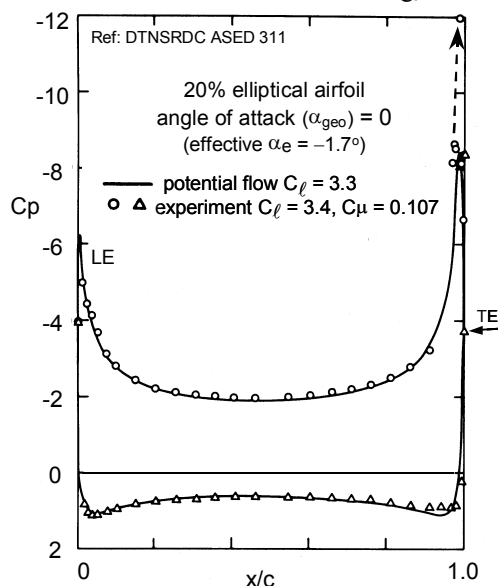
Figure 3. Comparison of calculated (inviscid) and experimental pressure distribution for a CC airfoil, C_L is specified as a replacement for the released Kutta condition.

developed by CC is centered around midchord, with the leading and trailing edge stagnation points both moving equally, which corresponds to load arising at ¼ and ¾ chord (c) locations. As lift is incremented by slot flow, there is no lift-induced downwash on a two-dimensional (2D) foil to cause a change in *effective* angle of attack, which is why the leading edge stagnation point moves in complete concert with the one at the rear. In contrast, for a finite span wing the vorticity created by the spanwise load variation produces a downwash velocity which effectively causes the wing sections to operate at the 2D equivalent of an ever-increasing negative incidence as lift from blowing is increased (Prandtl's lifting line theory, Eqn. 2). The consequence of this *induced* angle of attack is a reduction of the load centered at ¼ chord, with no impact on that developed at ¾ c. As an example, for an augmented lift coefficient (C_L) of 1.5 at zero geometric angle, lifting line theory for elliptic loading shows that an AR=2 wing section would be operating at a –14 deg effective angle-of-attack (Eqn. 3).

$$\alpha_i = -C_L / \pi AR; \quad C_L/\alpha = 2\pi AR / (AR+2) \quad (2)$$

$$\alpha_e = \alpha_{geo} + \alpha_i = \alpha_{geo} - C_L / \pi AR \quad (3)$$

$$C_L/\alpha = 2\pi AR / ((AR^2+4)^{0.5} + 2) \text{ (Helmbold)} \quad (4)$$

The change in effective incidence modifies the chordwise pressure distribution with the result that it is reversed in comparison to operating at the same C_L obtained in the conventional manner with pitch angle, see Figure 4. The induced angle-of-attack due to the net lift has caused an offset of the leading edge stagnation point location that mostly nullifies the movement produced by augmented circulation. Effectively, the front-half of the lift-due-to-blowing is lost because of the negative circulation increment produced by downwash. Note: it is a coincidence that for an aspect ratio of 2 the downwash offsets the effect of augmented lift by a factor of one-half. Theoretically, this makes for an absence of a leading edge pressure peak at all blowing levels when the AOA is near zero; a leading edge gradient will arise in response to non-zero pitch angles.

Inviscid computational solutions provide additional insight into the general nature of the flow field, even though they cannot identify the required slot flow rate. Figure 5 illustrates the flow features on the underside of the wing trailing edge at conditions corresponding to a moderate Cμ. In this lifting surface panel-method solution (VSAERO, AMI), the CC effect is simulated by specifying the wake separation location (95.5%c); the slot discontinuities are faired-over. (For

confirmation of the wake location, an extremely large wing span of AR>50 can be specified to ensure that the desired experimentally demonstrated airfoil C_ℓ is being
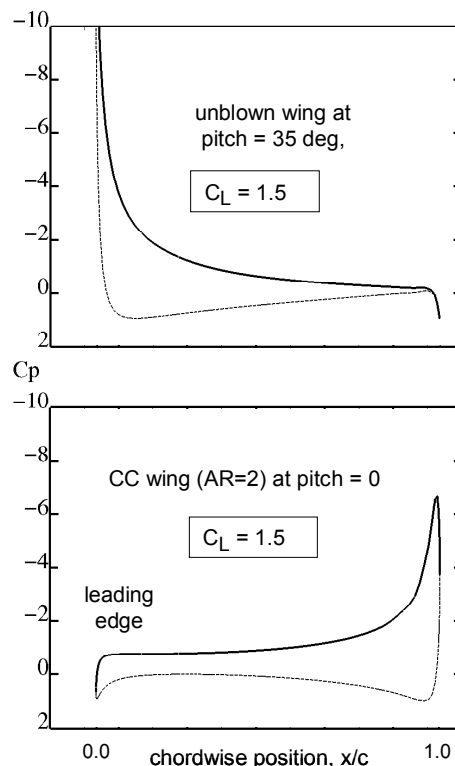

Figure 4.   Comparison of mid-span pressure distributions for a conventional lift wing with that of a CC wing at zero pitch angle; downwash eliminates the leading edge pressure gradient of the CC wing, for aspect ratio =2. (VSAERO panel code, inviscid).

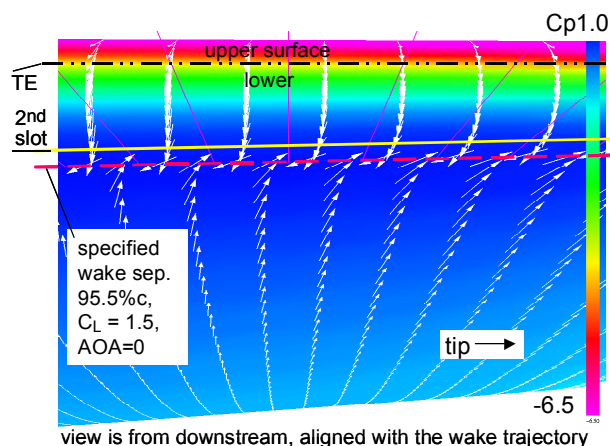view is from downstream, aligned with the wake trajectory

Figure 5.   Aft underside perspective of the theoretical conditions in the trailing edge region, vectors indicate flow direction. The solution does not directly include a jet, only the resulting C_L. 20% t/c elliptical cross-section, AR=2. (VSAERO)

4

modeled.) The high suction region extends to and slightly onto the lower surface, followed by a rapid recovery to stagnation pressure; the pressure profile in Figure 4 is from this same solution. The pressures are a result of the circulatory lift and not due to local influence of the wall jet because the jet as such is not present in the computation. The formation of the finite-wing vortex sheet that defines the wake attachment location is evident from the flow direction vectors. For this case where $C_L=1.5$ at zero pitch angle (compared with the maximum C_L of about 1.25 available from a conventional appendage), the location of the wake stagnation point is about 1%c forward of where the second slot would be on a dual slotted configuration.

Potential sources of adverse effects of a small aspect ratio wing that are unique to CC arise from the tip vortex formation location. For a lifting CC wing of AR=2 at zero pitch angle, there is little or no pressure differential between the upper and lower surfaces near the leading edge to cause the tip vortex to begin forming in the same location as on a conventional wing (Fig. 4). Not until about the 80% chord location does an appreciable differential occur. The largest gradient is normally found near the slot location, providing an opportunity for a local mutual interaction between the wall jet, lower surface flow merger (stagnation zone), and tip vortex formation.

Whereas the aft location of the tip vortex has the potential for disruptive effects, there is an influence that could be of some benefit. Figure 6 shows the spanwise component of velocity on the upper surface, as an indicator of the extent of local 3D conditions on the planform. For lift developed by CC, there is much less of a general spanwise velocity component, as compared to the same lift developed by pitch angle. Wing surface flow direction is more 2D-like.

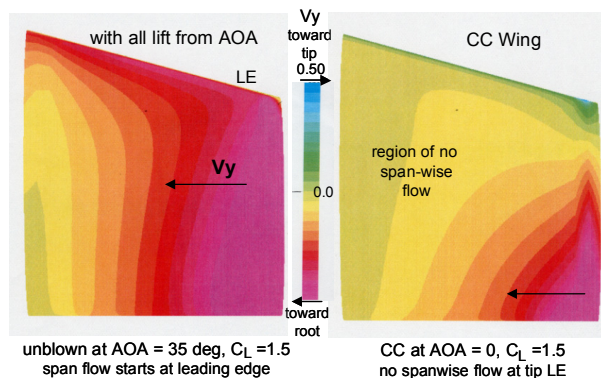A related consideration is whether the non-uniform chordwise induced velocity created by a low aspect ratio lifting surface at high lift would significantly alter the CC performance versus that of the two-dimensional profile (airfoil). That is a question of lifting line versus lifting surface theory. The lifting line concept is predicated on a chordwise uniform induced velocity, which is considered adequate for representing conventional performance down to at least an aspect ratio of 4.

There is another 3D effect unique to CC. In static freestream conditions it has been observed that the jet flow near the termination of a slot is highly skewed toward the low pressure region produced by the Coanda flow inboard of the slot termination. There has been some evidence of a sheet roll-up at the slot inboard and outboard ends. Thus the slot itself may have a finite-span effectiveness factor.

Limits to Circulatory Lift of Finite Span Wings

In the 1950's the newly recognized ability to develop high lift coefficients using the jet-flap effect led to discussions on whether there were limits to circulatory lift brought about by the vortex system of a finite wing. The consensus was that the severe vertical displacement of the trailing vortex sheet at high C_L would not only cause the usual vertical downwash but would also cause a component of inflow that subtracts from the incoming free-stream velocity, that is, a tilt of the induced velocity.[5] Therefore, a limit in C_L was expected and would have the most impact at low aspect ratio. Compared to the jet-flap, CC can more readily approach whatever limits that may exist; accordingly, it is appropriate to examine the theoretical derivations in the literature. Davenport provides a review of the three published articles on the subject.[5] A limit to circulatory lift, C_{L_Γ}, (excludes any jet reaction force contribution) is reported as a linear function of aspect ratio (Fig. 7). There are three different assessments of the value for the linear constant, differing by more than a factor of

Figure 6. Comparison of *spanwise* flow distributions on upper wing surface for two different sources of lift at identical C_L. (VSAERO)
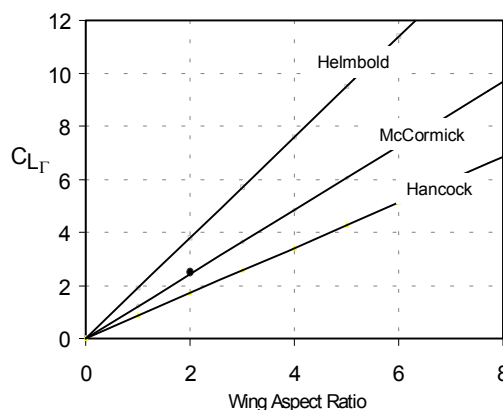

Figure 7. Theoretical circulatory lift limits for finite span wings as predicted by several theories.

two. The most pessimistic derivation would give a C_L limit of 1.7 for the hydrofoil planform of interest; the most optimistic would give 3.8, with the third one indicating a C_L of 2.4. This third value—given by McCormick's analysis—is recognized to have a weakness in the theoretical modeling, however, it is reported as correlating quite well with jet-flap data. The lowest limit (Hancock), if valid, would impede the CC appendage concept. Hancock's projections are exceeded by jet-flap results and so should be questionable, unless as he points out, the strong momentum flux in the jet-flap wake might have mitigating effects. The most optimistic assessment (Helmbold[6]) is perhaps the most rigorous theoretically and gives a result that would just allow a CC appendage to take full advantage of the demonstrated performance of CC airfoils. If valid, the remaining question is how close to the theoretical limit is it possible to approach in practice and what non-linear behavior would result.

For the stated reasons that differentiate a small aspect ratio CC wing from the thoroughly investigated applications to high aspect ratio, the current project was initiated to determine if performance could be accurately predicted using the same fundamental principles that apply to conventional wings.

Performance Prediction

A pre-test prediction was made for the hydrofoil performance based on classical wing theory and the known characteristics of the proposed parent CC airfoil profile.[7] Subsequent comparison to water tunnel test results would then reveal any significant finite wing issues unique to CC.
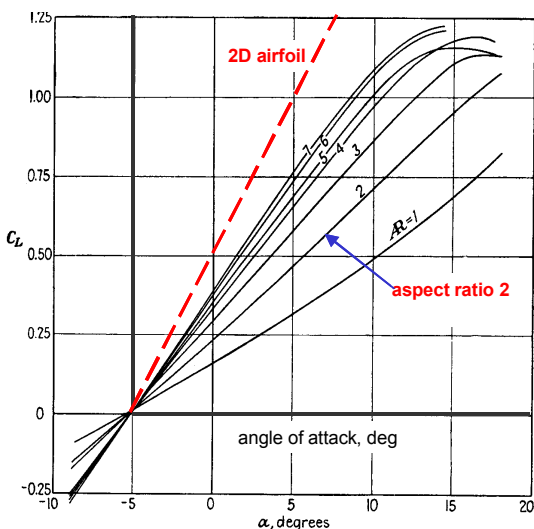

Figure 8. Aspect ratio effects for conventional wings, a reduction in C_L-AOA slope (Prandtl's data).

Figure 8 is the familiar data from Prandtl that reveals how the lift curve slopes of conventional wings are influenced by aspect ratio. At a given angle, the wing lift can be less than half that of the airfoil. These changes in the rate of response to AOA conform to finite wing theory and are a consequence of the induced angle of attack resulting from downwash produced by lift. The same finite wing theory was used to make the performance prediction for the CC wing, using the notion of a 'load line', which simply represents how induced AOA tracks wing lift in accordance with lifting line or higher order theory (Eqn. 2-4). Figure 9 shows the performance map of the CC airfoil for lines of constant $C\mu$.[7] Overlaid on the data plot is the wing load
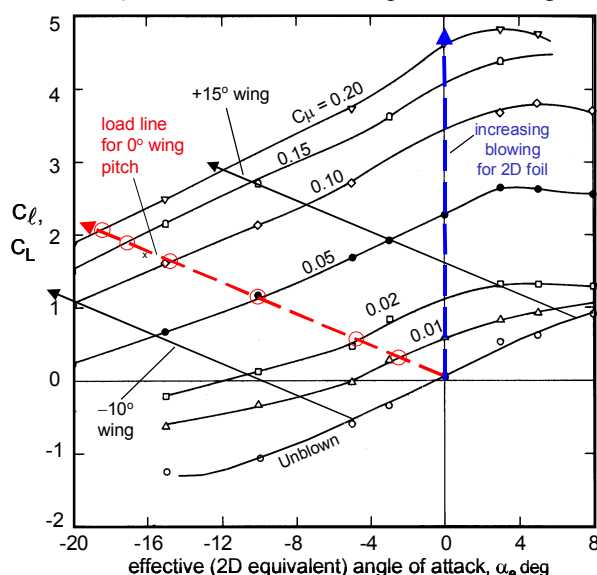

Figure 9. Performance map of the parent CC airfoil with wing load-lines (α_e vs C_L) super-imposed for AR = 2. ($\alpha_e = \alpha_i + pitch$)
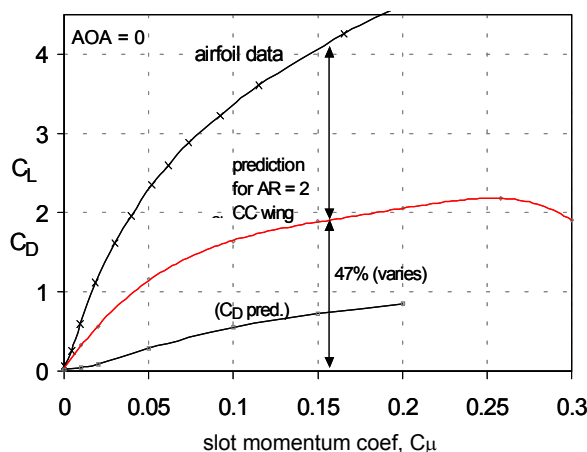

Figure 10. Predicted performance of the hydrofoil. Reduction from the airfoil curve is about same as for C_L vs AOA on a conventional wing of equal AR

line at zero pitch for AR=2. The relationship used is $AOA = -9*C_L$, depicting that the effective 2D equivalent AOA declines at a rate of 9 times the wing C_L (Eqn. 2).   Points of C_L versus C_μ as read from Figure 9 where the load line crosses lines of C_μ are plotted in Figure 10.   This mapping technique for airfoil-to-wing captures any non-linear behavior of the airfoil (wing) section, with a high degree of validity if the planform is reasonably close to having a uniform downwash angle. Figure 10 shows what is now the expected lift performance curve for the CC wing, based on the assumption that it is impacted by finite span effects the same as for a conventional wing.   In comparison with the airfoil performance at a constant effective AOA of 0 deg, the average decline in C_L is about 53%. Drag is predicted based on the conventional drag polar equation, using a conservative estimate of the Oswald span efficiency factor for a rectangular wing.

MODEL AND EXPERIMENTAL SETUP

The hydrofoil model cross-section contour is generally similar to that used in early CC investigations in the United Kingdom.[8] The distinction is in the details of slot placement, nozzle design, and ejection angle, as the current model reflects a number of years of experience with CC airfoils.   The design is a minor variation of the one evaluated in Reference 7.

Model Design

A summary of the geometry of the 2-foot semi-span model is presented in Figure 11 and is sufficiently detailed to allow replication of the functional components of the tested profile. The planform has a leading edge sweep angle of 15 deg with an effective (reflective) aspect ratio of 2 to resemble those currently in use for sternplanes and rudders. The sweep angle corresponds to a chord taper ratio of 0.76. Depending on the intended application, the linear scale factor is about 15%. The cross-section profile is basically an ellipse, with the thickness ratio of 20% being somewhat larger than for a conventional appendage. Upper and lower surfaces are identical and independently functional for ejection of mass over the rounded trailing edge. See Figure 12 for assembly views.

While the potential application is similar to that addressed in Reference 9, the current model is directed more toward an exploratory investigation rather than to a specific application, hence there is no tailoring of the design to accommodate any particular usage.   A consideration was to make the geometry specifications as simple as possible, for ease of post-construction contour verification and for future CFD correlation efforts.

There is currently no adequately validated computational method (CFD) to assist in the design of a true CC airfoil, where there is a fully rounded trailing edge. The absence of any contour feature that helps to fix the detachment point of either the upper or lower surface flow exacerbates the turbulence modeling issues. Potential-flow solutions using the anticipated lift coefficients are an economical way to examine
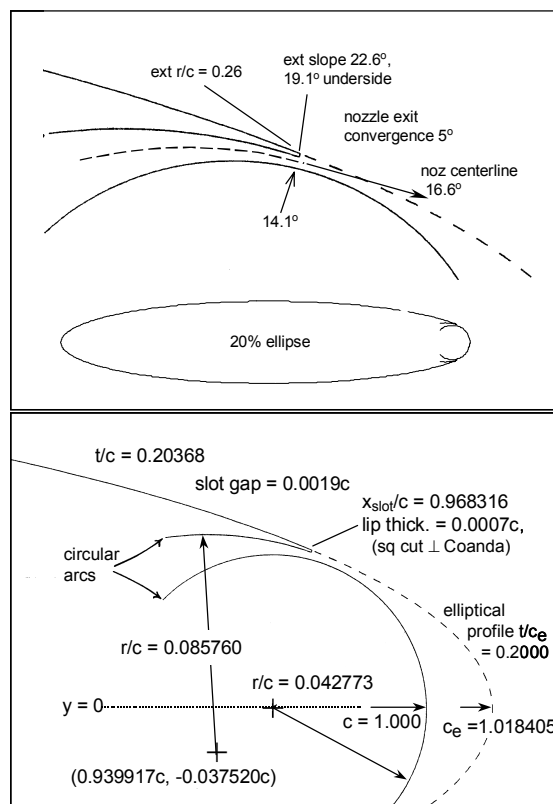

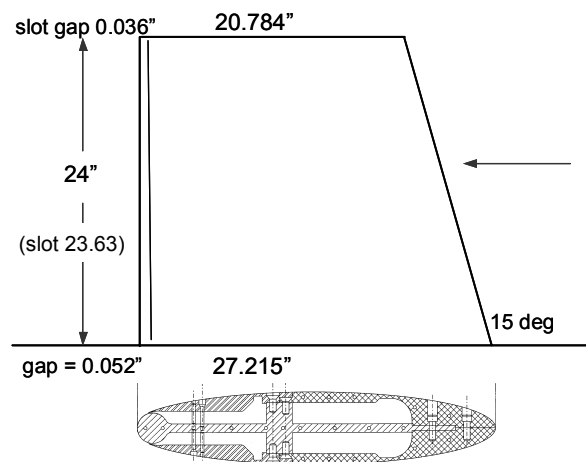*Figure 11(a). Trailing edge design details.*

Figure 11(b). Planform geometry, mean chord of 24 inches, effective aspect ratio of 2.

chordwise load distributions for the selection of thickness and camber for augmented lift airfoils. For guidance of design details, there is only the historical database of what has worked well in the past and what should or must be avoided.
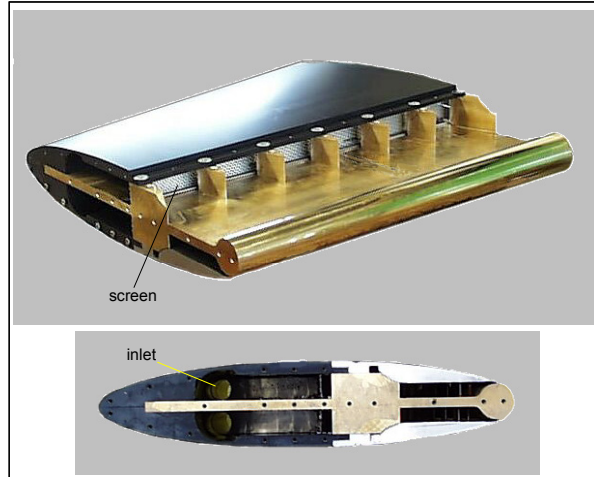

Figure 12. Interior views with tip cover and slot plate removed.

The simplicity of the CC section design used in this investigation, two circular arcs and an ellipse, must not be taken to mean that the performance potential of CC can be obtained in a cavalier manner. There are a number of lessons-learned practices that went into constraining the design shown in Figure 11, which is why the surface slope angle details are noted. The angles are included here not as a guideline, but as a baseline reference for comparison with future designs. Of particular importance is to have a fully convergent nozzle, with enough of a contraction angle to ensure that fabrication tolerances, hand finishing, re-work mishaps, and slot gap expansion under pressure will never result in a non-converging exit. Nor is any kind of obstruction to be designed into the nozzle, as in a structural support. Slot position, ejection angle, and positioning of the Coanda surface with respect to the unmodified foil contour are among other parameters to receive attention.

The wing section profiles are non-dimensionally identical along the span, except for a small taper in slot gap. The gap to chord ratio decreases by 10% in the outboard direction to offset the finding for this model that the model interior (duct) pressure increased almost linearly root-to-tip by about 5%. The objective was to have a nearly constant spanwise $C\mu$, without any chance that $C\mu$ would be higher outboard so as not to make the tip vortex even stronger. There was no intent to taper the gap for an elliptic load distribution which, when combined with a simple flat tip cover plate, was recognized as making for a strong tip vortex at high lift. Operational designs would be

directed toward the management of vortex strength and core intensity. The mean gap setting of 0.0019c was selected based on remaining well within the range of airfoil experience. Seven pairs of push-pull screws are provided to set the gap, with plastic thickness gages used in the procedure for what is judged an overall setting accuracy of 0.0015". The slot adjustment setting was not changed in the course of the test. Gap expansion at the peak internal pressure of 34 psi was about 8% as determined by a dial gage, which compares favorably with a structural analysis.

Model Fabrication Notes

Due to the required location of the load cell, the slot flow was supplied through a small inlet pipe located against the forward wall of the interior (Fig. 12). As was not unexpected, a racetrack cavity flow pattern occurred in the model interior. The consequence was that both a spanwise component of velocity and a spanwise pressure gradient existed within the slot feed duct; plenum-like conditions would have been preferable for a research model. The spanwise duct velocity convected to the exterior, causing skewed slot flow in a direction of tip to root. Although provisions for a contingency retrofit of an internal distribution manifold had been made, scheduling requirements necessitated using only a flow damping screen, of 30% free area, Figure 12. The velocity approaching the screen is estimated as 6% of the slot exit velocity. There remained about 5 deg of skew from the nozzle in most portions of the span, along with some remaining gradient in the spanwise pressure as measured at the nozzle exit. The pressure gradient was compensated for in terms of $C\mu$ by slightly changing the slot gap distribution. The angling of the jet sheet is not seen as having a performance impact, but should be a topic of a future investigation with a 2D model because the application of CC to rotary blades, or single-end feed of fixed devices, will inherently produce some degree of skew.

Model contour fidelity was verified with special attention directed to the trailing edge region. The Coanda surface was fabricated from brass, which was found to be softer than might have been expected. The final hand finishing of the brass surface resulted in less than a smooth polished surface, there were scratches and file gouges. This is mentioned to make the point that the CC function does not necessarily require laboratory grade precision surfaces, as concluded from the model meeting or exceeding performance expectations. In static flow, using air and sweeping yarn tufts spanwise along the Coanda surface for visualization, no wakes could be detected from the internal structural components. With water flow into

air, however, patterns could be seen in the water sheet that corresponded to the slot adjustment screw locations.

Facility and Experimental Setup

The investigation was conducted August – September 2002 in the NSWCCD Large Cavitation Channel (LCC), a water tunnel of 10-ft x 10-ft cross section in Memphis, TN.[10] Test section static pressure is controllable for the purpose of cavitation investigations and LDV flow field survey instrumentation is available. Reynolds number based on mean chord was 2.1 million at the usual test speed of 10 fps, dynamic pressure (q) of 97 psf. No flow transition trips were used.

Using a wall standoff plate to serve as a reflection plane, the model was mounted on a load cell balance. See Figures 1 and 13. In order to verify any unusual balance reading trends, as well as for other purposes, two surface taps were used to measure the pressure differential at the center of the wing.

Valving outside of the tunnel test section permitted allocation of flow to each of the two slots. Model interior pressures of up to 34 psig were set by a variable speed motor-pump, with an option to use computer control to automatically step through the pressure range. Pressure in each duct was recorded at a single interior span location, 41%s. As is customary in the literature, the experimental value of momentum coefficient $C\mu$ is determined from measured slot mass flow rate and a calculated jet exit velocity based on the duct pressure relative to free stream static pressure. It is recognized that the true jet velocity is not known, since the local static pressure at the slot exit is not really free stream static and varies with C_L and other factors.

Slot flow rate was measured by a precision turbine flowmeter with an operating maximum-to-minimum ratio of 15. The flowmeter capacity was sized to the test plan requirements so that this full turndown range of 15 was usable and there was no need for a second flowmeter to extend the coverage range. Validity of mass flow and slot pressure readings was continually monitored by using the readings to back-calculate the apparent slot exit area, a parameter that will remain with the test data sets. The comparison of measured to calculated flow rate also reveals the difference between actual and theoretical V_{jet} (that is, the difference in P_{local} and P_∞), once slot gap expansion under pressure has been quantified. This comparison reinforced the point that it is necessary to actually measure slot flow rates, because theoretical calculation from duct pressure will produce a non-linear bias in the performance data (not shown).

Each of the two slot feed tubes passed adjacent to the load cell. Care was taken in the design of the

plumbing lines to minimize pressure tares, which were measured by sealing the slots and sweeping line pressures up to 20 psi, both collectively and individually. The tares were found to include some minor effects on certain moments.
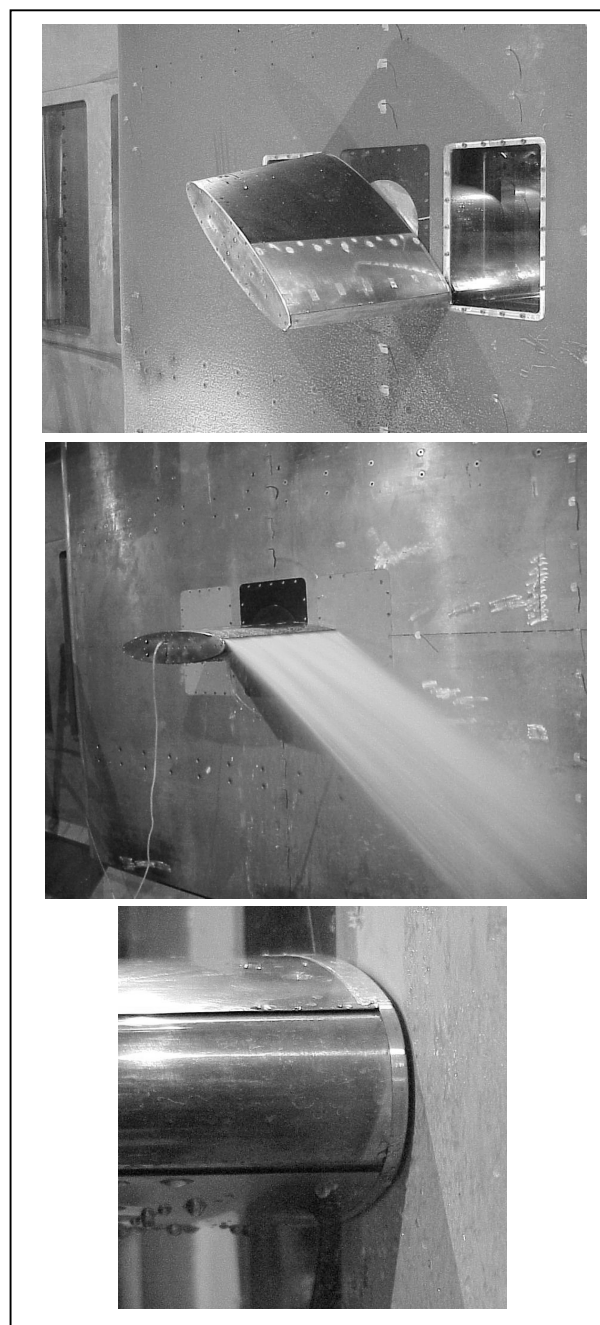

Figure 13. Installation of the 2-ft model in the NSWCCD Large Cavitation Channel. (There is little or no Coanda-effect turning for water-into-air, as expected.) See also Figure 1.

Terminology

Reflecting the aerodynamic origin of the technology, the term "blown" is used to refer to the pumping of mass flow from the slot. Unblown refers to a shut-off of the slot supply line by closing a valve, which is in contrast to turning off the supply pump but allowing the line to remain open (can result in a slot outdraft).

Data

The location of the single available duct pressure tap upon which calculation of V_{jet} is based did not give a reading equal to the mean spanwise pressure, as measured at the slot exit. The duct tap reading was approximately 2% lower than the mean pressure. Consequently, the presented $C\mu$ values are about 1% lower than that of the average spanwise conditions.

The single flowmeter was placed in the supply line upstream of where the line branched to both slots. Since the slots were verified as having the same effective exit area, whenever simultaneous blowing was being used, the flow rate in the calculation of $C\mu$ for each slot was allocated in proportion to relative duct pressures. That procedure is completely adequate for what had been the planned investigations of dual blowing. In the course of the test, however, interest developed in very low relative flow rates from the second slot. For that situation, the prevailing positive pressure in the unblown slot duct--presumably from pressure recovery from the blowing slot--made for a bias in the duct pressure reading. The consequence is that a duct pressure based allocation of flow rates credits an excessive momentum to the second slot when the relative fluxes are the order of about 4% or less. When low percentage rates are quoted in the following discussions for dual slot usage, the actual percentage could well be much less.

Both upper and lower slots were separately activated at positive and negative pitch angles, but not in all combinations. Pitch angle (AOA) convention was for nose-up to be recorded as positive, no matter which slot was active. The use of the lower slot while at positive AOA corresponds to a negative incidence relative to the airfoil databases. For some analysis perspectives, it is appropriate to view all data as if from an upper slot configuration, with the sign of AOA, C_L and moments changed accordingly, which is justifiable once the model has been shown to have symmetric performance.

STATIC FLOW CHARACTERISTICS

Static conditions--meaning zero freestream velocity--are of interest for both the insight offered into active flow control phenomena and the relevance to the maneuvering of VSTOL aircraft and naval vessels at extremely low speed. It is also one means of relating the CC design to profiles used by other researchers in basic jet flow investigations.

Static Flow with Dual Slots: Thrust Vectoring

Figure 14 consists of photographs taken during an initial checkout of the assembled model using air, with tufts for flow visualization. Single slot blowing shows the usual 180 deg turning that is expected from the Coanda effect. When dual slot blowing was examined, the yarn tufts showed that the two wall jets merged to form a single free planar jet that could be adjusted to any angle. The smoothness of controlling the angle, the spanwise uniformity, and the sharp definition of the free jet sheet were remarkable.

In the filled water tunnel, to quantify the effectiveness as a potential static thrust vectoring

single slot blowing (lower)
180 deg redirection of the wall jet

initiate dual slot mode
very low pressure in upper slot

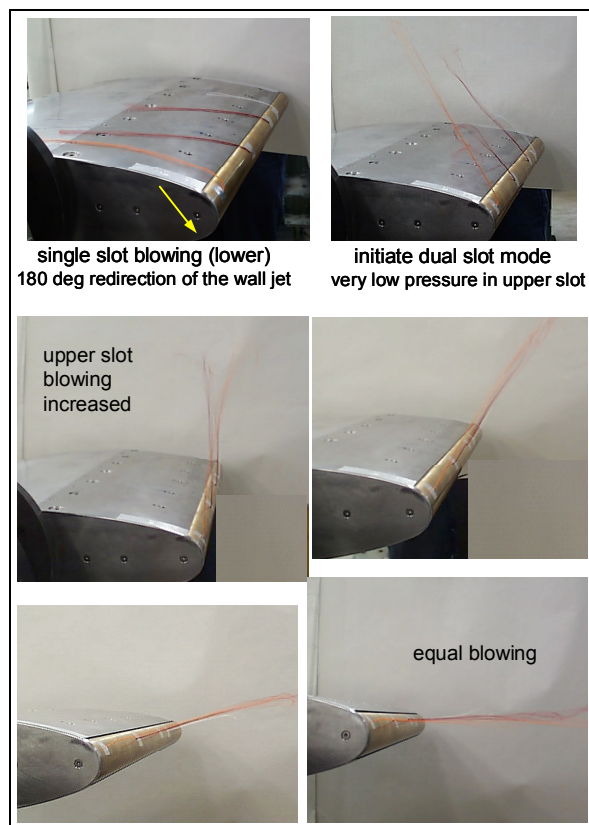upper slot blowing increased

equal blowing

Figure 14. Visualization in air using tufts shows merger of the two wall jets into a spanwise uniform free planar jet, controllable to any angle by differential pressurization of the slots.

device, the ratio of slot supply pressures was varied under quiescent tunnel conditions while the resultant force components were measured by the load cell. The results of converting the forces into a thrust angle are shown in Figure 15 as a vector diagram where vector length is the ratio of measured to the ideal theoretical thrust, based on the flowmeter and duct pressure readings. A full 0-360 deg vectoring range was available, just as seen in the tuft visualization. Reaction force efficiency ranged from 70 to 80%, depending on the vectored direction. The thrust angle bears a simple mathematical relationship to the relative momentum flux. The empirical equation, plotted in Figure 16, calls attention to the sensitivity of surface lift-off of a fully turned Coanda wall jet to low pressurization of the second slot.
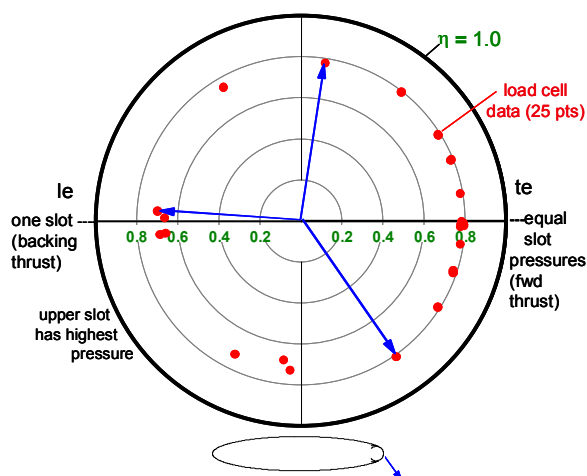

Figure 15. Vector diagram of static thrusting force data (water tunnel), depicted as the direction of the merged slot flow; full 0-360 deg obtained with 70-80% thrust recovery.
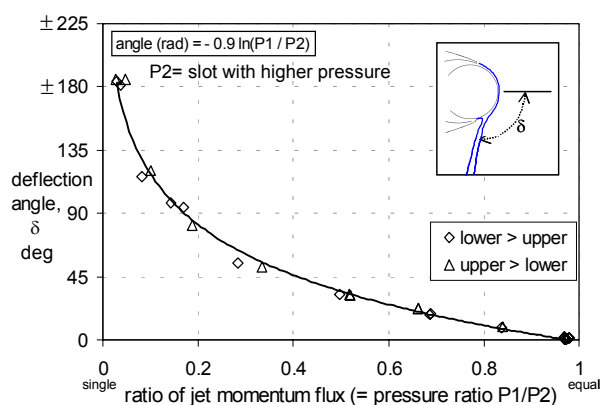

Figure 16. Static thrust angle as a function of relative slot momentum flux (pressure ratio), presented as the direction of the merged free jet.

This static omnidirectional maneuvering force capability at a reasonable level of efficiency is an unexpected finding and becomes a supplemental virtue of a CC control surface for naval hydrodynamics and VSTOL aircraft applications. As for operational applications, the experiment described above was conducted without an ambient velocity, other than that induced by jet entrainment. No determination was made of the vectoring angle capability in presence of a vehicle drift speed. If the effect of an oncoming flow field is equated in some manner to the issuance of a weak jet from the second slot, then it can be assumed that the control range would be less than the full 360 degrees. With forward speed, vectoring the merged jet to 90 degrees to make it perpendicular to the wing chord would provide a jet-flap mode of operation to supplement the high efficiency CC mode in certain situations.

References were found that can provide additional data and insight into the properties of dual jets. The phenomena of wall jet merger and conversion into a free jet were examined in detail by Rew over a limited deflection range.[11] Reference 12 presents a comprehensive survey of the flow field of a static configuration much like that of current interest. The application was to a variable angle jet-flap device, the Honeywell VDT, which was considered for use on helicopter rotor blades[13] and aircraft rudders. In Reference 14, static thrust control on a CC wing using a different implementation of opposing dual slots was demonstrated with an efficiency of 67%.

The Question of Coanda Surface Static Thrust Gain

The model setup in the LCC also permitted an investigation of a question regarding the Coanda effect: is there a static thrust gain, as might arise from mass entrainment associated with turning a wall jet around the half-circle cylinder that comprises the trailing edge? The approach was to keep the experimental arrangement exactly the same while changing nothing more than the extent of the jet turning angle, simply by switching the ambient fluid in the tunnel. For water-into-air, there is minimal jet turning due to the mismatch in fluid densities, only about 15 deg beyond the nozzle angle of 17 deg. Thrust recovery is 88%, Figure 17. The experiment is then repeated with the test section filled with water to 'activate' the Coanda effect. The usual 180+ deg turn now occurs, as determined by forces on the load cell. There is no thrust increment associated with enabling the additional 153 degrees of turning, as is consistent with reports in the literature.[2] An ejector or shroud arrangement would be necessary for augmentation of static thrust, as there is no source of

flow energy in the exterior field to leverage as a means of developing a control force.
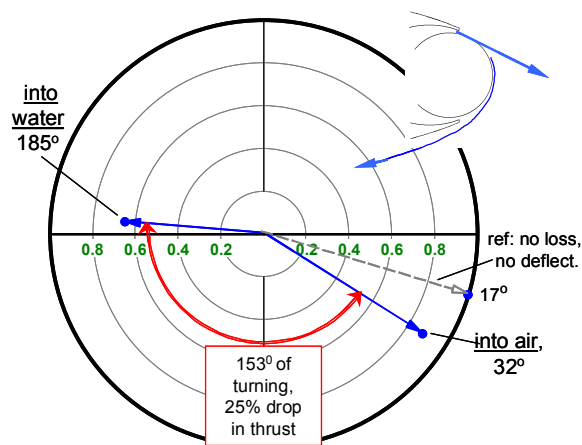

Figure 17. Influence of turning angle on static thrust of a Coanda surface: comparing water-into-air (little deflection) to water-into-water (full turn).

Axial Static Thrust Efficiency

With dual slot water ejection into *air*, the thrust recovery is 71%, notably lower than the 88% found with a single slot. The explanation is that the two water sheets do not merge into a directionally coherent sheet in air but rather fan out into a spray. With a homogenous environment of all water, the static dual slot thrust recovery is higher, at 80%, as was seen in Figure 15. This efficiency can be compared to the 84% found by AMO Smith[15] for a dual slotted 2D profile where the objective was that of a propulsive wing, termed a 'power profile'. As explained in Reference 15, which refers to a basic study by Wygnanski, a component of thrust loss results from entrainment effects reducing the local pressure on the trailing edge.

UNBLOWN LIFT

Figure 18 presents the unblown lift coefficient as function of pitch angle, with only the positive angles shown, for a Reynolds number (Rn) of 2.1 million based on mean chord. The lift curve slope is 0.047 per degree, which is very close to that predicted by lifting surface theory. Stall angle is 26.5 deg as determined by fine increments in AOA (not shown) and the sharp stall correlates with a nose-down pitching moment change. Maximum lift coefficient C_L is 1.16, unblown. Lifting line theory would give an induced angle of 11 deg at maximum C_L, making the effective AOA at stall to be 16 deg. This effective stall angle is in general agreement with the airfoil data of Reference 7. The

rolling moment indicates the 47% span location as the center of lift, while the pitch center is 0.230c forward of the root center.

For comparison to a conventional appendage, Whicker[16] gives the following data at the same Rn and aspect ratio for a NACA 0015 wing with a taper ratio of 0.45: lift curve slope = 0.045, maximum C_L=1.24 at stall angle of 27.5 deg. The NACA 0015 has a larger leading edge radius than that of the CC hydrofoil, 0.025c versus 0.020c.
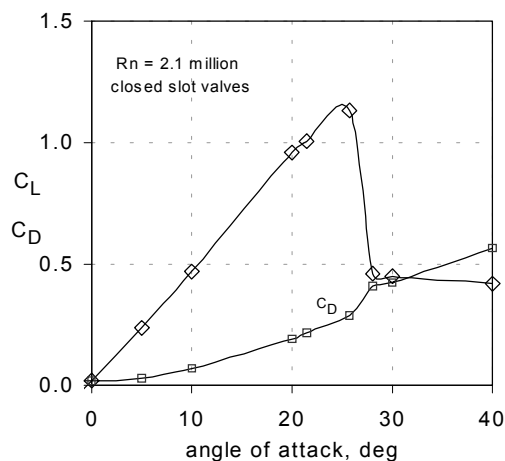

Figure 18. Model performance when unblown, stall angle of 26.5 deg.

LIFT WITH CIRCULATION CONTROL

The presence of the fully open unblown lower slot was not detrimental to the lift augmentation produced by the upper slot, as determined by carefully fairing over the lower slot with metal foil tape and finding no difference in basic performance. Performance of the two slots, used individually, was identical, thus confirming the symmetry of the model fabrication and slot gap setting. The identical performance was particularly meaningful in that one nozzle/Coanda surface had received accidental abuse during checkout of the pumping system, an unplanned demonstration of robustness. Confirmation of symmetry permitted the occasional expedient of setting the condition of a negative pitch angle by keeping the model at positive pitch and switching which slot was fed by the pump.

Initial Findings and Extension of Lift Capability

Figure 19 depicts one of the first pressure sweeps to examine the response to slot flow, at a constant geometric AOA of zero deg. The lift augmentation ratio in the initial linear portion of the

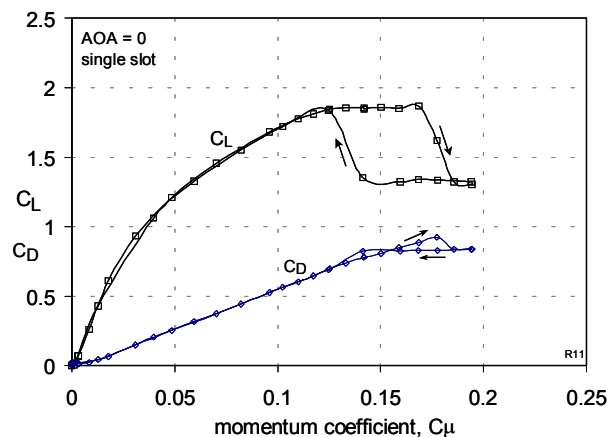curve is 36, somewhat better than expected as it corresponds to the 2D equivalent of about 70 or more,

Figure 19. Lift response to single slot blowing at zero angle-of-attack, with earlier than expected lift limit and hysteresis.
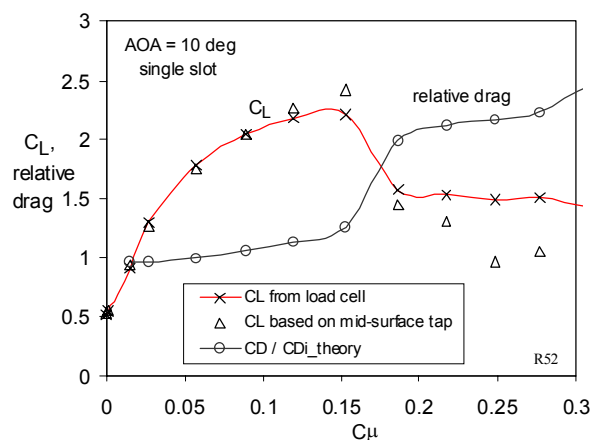

Figure 20. Diagnostics of the early lift-limit: drag relative to lift increases, planform center pressure differential deviates from load cell lift readings.
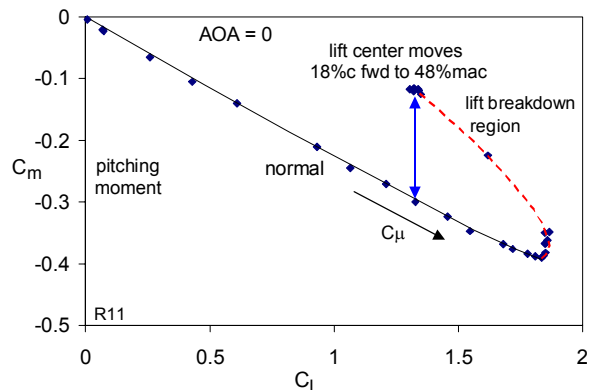

Figure 21. Diagnostics continued: model pitches up when lift reaches limit.

which is above average for an uncambered airfoil. The transition from a linear to a square-root like response to $C\mu$ is also as projected. What is unexpected is the lift roll-off at a $C\mu$ of only 0.12, which had been anticipated to occur at double that value, if at all. Associated with this lift limit is a large hysteresis loop. The situation was identical for each slot, and was found at other pitch angles.

Figures 20-21 show how the balance load readings were used to help identify the causative phenomena associated with lift roll-off (the model did not have chordwise or spanwise pressure taps). The lift roll-over correlates to a sudden rise in drag as compared to expected levels based on the lift-induced drag (C_L-squared). Revealingly, a large nose-up pitching moment develops with the center of lift moving forward by $18\%c$ for the same C_L, Figure 21. The center of lift change cannot be attributed to leading edge separation, since as shown in Figure 4 there is no expectation of a pressure gradient. There is also a divergence in the correlation between mid-model pressure differentials and loads registering on the balance (Fig. 20). The profile of the pressure distribution on the model is thus assumed to begin to depart from that given by inviscid theory, which CC normally follows quite well. There was only a very minor change in the spanwise center of lift and nothing unusual happened to yaw moment versus drag, hence this is not a phenomena unique to one end of the model. The tentative conclusion based on similarities to experiences with airfoils is that the wall jet is turning onto the lower surface and penetrating too far forward before separating and turning into the cross-flow. The result is reduced pressure on the end-of-chord region (the drag rise) and reduced pressure on the aft underside (the lift reduction and pitch up). The above-described condition has been seen to some degree on a number of CC airfoils (Fig. 22), where it was identified from the surface pressure tap readings and the drag trends.[17] This phenomenon is not due to premature jet detachment, it is quite the opposite of that and has been referred to as "trailing edge pressure drawdown". It is not normally encountered at moderate blowing rates on a simple circular trailing edge airfoil design, therefore why it happened so early on this wing is unknown. No LDV survey was taken of the lift roll-over state since a means of eliminating the phenomenon was discovered in the course of the test and consequently there was a reduced priority for investigating the condition. Most CC trailing edge designs have been single slot, some with lower surface curvature distributions or tight radii such that adverse pressure gradients would result in jet separation without excessive forward intrusion; the requirement of dual-slot symmetry restricts these design options. For

reference, Figure 5 shows that the equivalent stagnation point location for the C_L where the lift limit began to develop ($C_L \approx 1.8$) would be forward of the unblown underside slot.
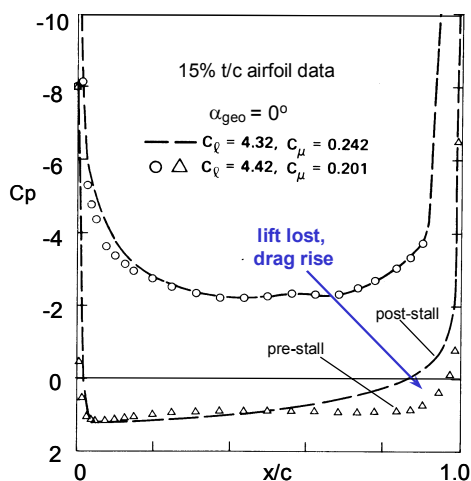

Figure 22. Probable cause of lift limit: "trailing edge drawdown" due to excessive turning of the wall jet, shown here occurring on a CC airfoil.

It was theorized that if excessive turning of the jet were the cause of the early lift limit, then perhaps using the lower slot to produce a counter flow would cause the jet to lift-off earlier, just as seen in the dual slot blowing experiments in air (Fig. 14). Therefore, a deviation from the test plan was made to explore mass ejection from the second slot while at the moderate to high Cμ's where the lift had declined. The results were immediate and dramatic: a full recovery to the expected curve of lift versus Cμ (Fig. 23). The drag, pitching moment, and mid-chord pressure differential also returned to expected values. The required second-slot momentum flux ranged from 2% to 5% of that from the primary slot, based on relative duct pressure. Figure 24 is an overall projection of the minimum requirement as a function of momentum coefficient (for Cμ up to 0.5), based on the limited dual blowing data obtained in the LCC. It is of interest that if the data in Figure 24 were plotted on a log scale and extrapolated to the high Cμ available at very low speed, the amount of second-slot momentum flux that would be needed is indicated as 19%, the same as required to produce 90 deg of deflection under static conditions (Fig. 16).

There is no performance penalty if a low rate of second-slot flow is applied at Cμ's below where it is needed (less than 0.10), except for the increased mass flow. It would be feasible, therefore, to incorporate a certain minimum ratio of slot momentum flux (~2%) into an operational valving system, even by simply cross-porting the appendage interior duct chambers.
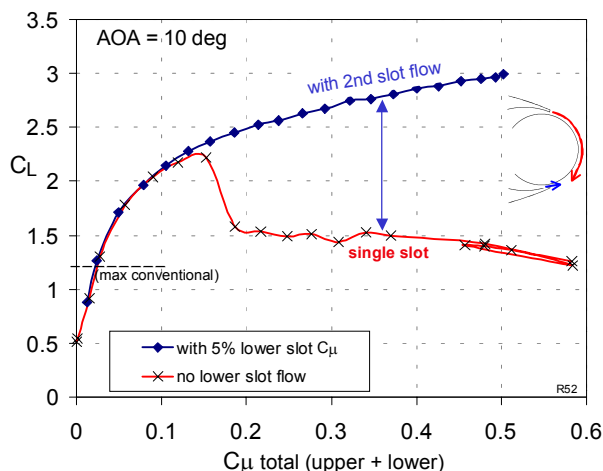

Figure 23. Elimination of the C_L limit: small counter-flow (5%) from the second slot used to influence the excessively turned jet (prevailing hypothesis).
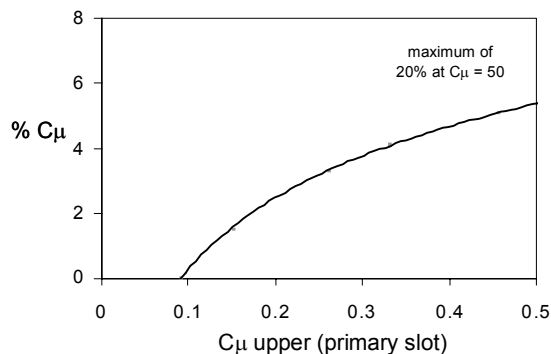

Figure 24. Required relative momentum flux from the second slot to extend CC performance gains to very high blowing coefficients.

Experiments with rates higher than required, up to a factor of 3, did not produce an appreciable further change in lift, indicating that the second-slot flow level is not critical, although there will surely be a point at which lift is adversely impacted. A brief examination of dual blowing on a CC airfoil (the LSB, unpublished) had dealt with only high relative flow rates from the second slot, which caused a lift decrement.

There is the question of why the single-slot lift roll-over condition occurred earlier than seen before, a 3D effect? Figure 25 shows that the use of a small end-plate delayed the onset of the lift limit. Sealing the unblown slot with tape caused a somewhat earlier occurrence, thus the lift limit is not due to a spanwise interaction with the unblown slot duct interior. CFD may eventually be able to provide some insight if the issues of turbulence modeling can be resolved. The ultimate explanation may well be different than that hypothesized here, but what is certain is that a slight
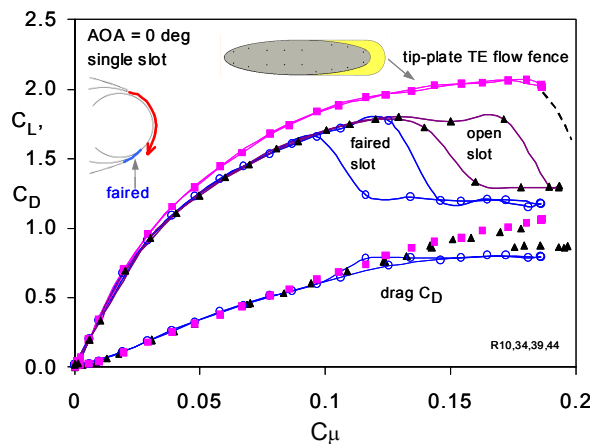
Figure 25. Influence of covering the unblown slot, and of a small tip end-plate.

Figure 26. Comparison of actual to expected performance.

counter flow from the opposite slot rectifies the situation. As to whether to call this earlier than expected single-slot limit a finite wing effect, the assessment is that not enough is known about the condition to make such a determination. In any case, since the basic concept of the CC appendage calls for inclusion of dual slots, using a small amount of bleed flow from the second slot as a remedial action means that it is not an issue for initial full scale application.

Comparison to Expected Performance

Figure 26 compares augmented lift to pretest predictions at a fixed pitch angle of zero degrees, where second-slot flow has been used as needed and included in the value for $C\mu$. The predictions were made as illustrated in Figures 9 and 10 where lifting line wing theory was used in conjunction with airfoil test data. The agreement is quite satisfactory, thus confirming that the impact of low aspect ratio on a CC wing is essentially the same as that on a conventional wing. More specifically, for the planform tested, the average value of C_L versus $C\mu$ is about 50% of that produced by the corresponding 2D airfoil, in the same ratio as the C_L versus AOA change on a conventional wing (Fig. 8). It can also be stated that the VSAERO panel method case for $C_L =1.5$ (Fig. 4,5) gave a C_L of 3.0 when the wing span was increased to AR=35 to approximate an airfoil, fully consistent with test results. Thus there is no indication of any basic effects of low aspect ratio that are unique to lift developed by means of the Coanda form of circulation control.

Because the trailing edge region details of the tested parent 2D airfoil differed somewhat from that of the hydrofoil, the precise ratio of 2D to 3D performance has some uncertainties. Therefore, it cannot be determined which variant of wing theory best fits the test findings, but the relationship is within the band of
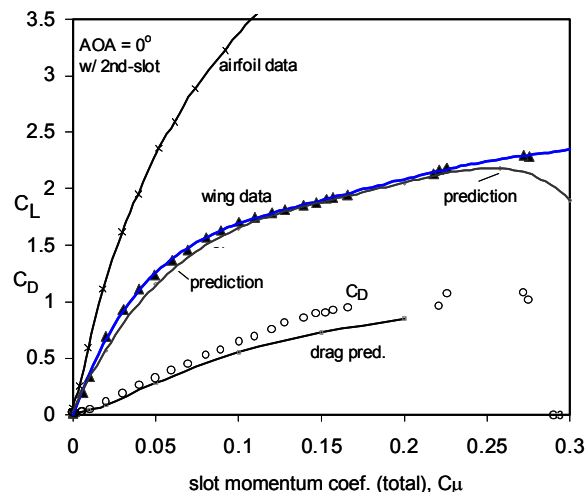
possibilities provided by Wessinger's lifting surface approximation, and Prandtl and higher order lifting line derivations. A combination of Prandtl's lifting line and Helmbold's higher order solution (Eqn. 4) was used in the general interpretation of the test results.

The control force capability of a conventional appendage was matched, without the need to pitch the CC hydrofoil, at a moderate $C\mu$ of 0.05 where the jet velocity ratio is 3.5 for the slot gap setting used. The additional lift that arises at higher $C\mu$ and with pitch angle is then an extension beyond conventional capabilities.

As for the theoretical limit to circulatory lift, Figure 7 includes the data point corresponding to the maximum demonstrated $C_{L\Gamma}$ in the LCC. It exceeds the derivation by Hancock and equals McCormick's prediction. Given that McCormick's derivation has a recognized weakness, we are left with Helmbold's analysis as expressing the plausible limit, and the CC hydrofoil is comfortably below it, leaving room for future growth through design optimization.

Angle of Attack Effects

Of the 11 pitch angles for which data was acquired, only three were with the benefit of second-slot blowing to eliminate the premature lift roll-over. Since those three displayed a linear behavior when plotted on a log scale (Fig. 27), and since the other angles were also linear up to the limit of single slot performance, it was considered justifiable to extrapolate the performance of the other pitch angles up to the highest $C\mu$ evaluated (0.50 for +10 deg AOA). Those extended results are presented in Figure 28 as a function of $C\mu$, and in Figure 29 as function of AOA for constant levels of $C\mu$.
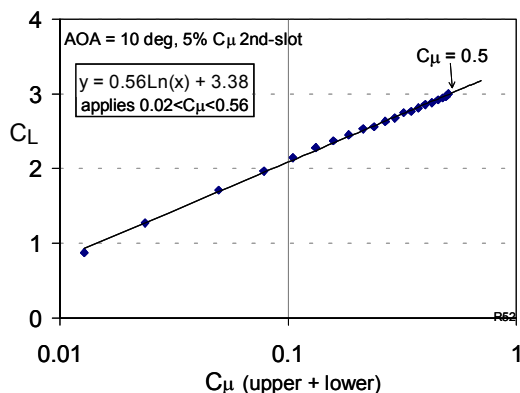
Figure 27. Typical logarithmic relationship between C_L and $C\mu$. Applies between the linear range ($C\mu < 0.02$) and the jet-reaction range ($C\mu > 0.56$).

For pitch angles in the range of –20 to +10, the C_L versus $C\mu$ relationship is very consistent (Fig. 28). A peak C_L of 3.0 was obtained in the test, more than twice that of a simple conventional control surface. Even when held to an angle of zero, the augmented lift at a $C\mu$ of 0.30 is C_L=2.3, double that of the maximum obtainable unblown C_L of 1.16.

The reduced lift gain rate at initiation of blowing for 20 deg, and to some extent for 10 deg, is as

expected, a consequence of aft separation (unblown) occurring before the upper slot location. Once the blowing has reached a level where the separation point has moved aft to the slot, the normal response rate to $C\mu$ is restored. (Separation when unblown, either at the leading edge or aft just before the slot, is a circumstance in which there is a recognized influence of Reynolds number on CC properties.) This behavior of the C_L versus $C\mu$ response matches quite well with what can be readily observed using the airfoil performance map and the graphical wing load-line concept, as a way to track effective-angle-of-attack effects. For example, in Figure 9 the reduced initial response at high positive wing angle can be traced by following the 15 deg load line from unblown up to $C\mu = 0.05$; compare it to the response found if starting at zero pitch. Correspondingly, construction of the line for –20 deg pitch would disclose the high initial augmentation ratio at that angle (Fig. 29). (All load lines are constructed by crossing at C_L=0 with the effective 2D AOA equaling the pitch setting; lift-due-to-blowing starts where the unblown curve is crossed. Data is available in the literature to enable synthesizing extensions of the CC airfoil map to wider ranges of angle and $C\mu$ levels.)

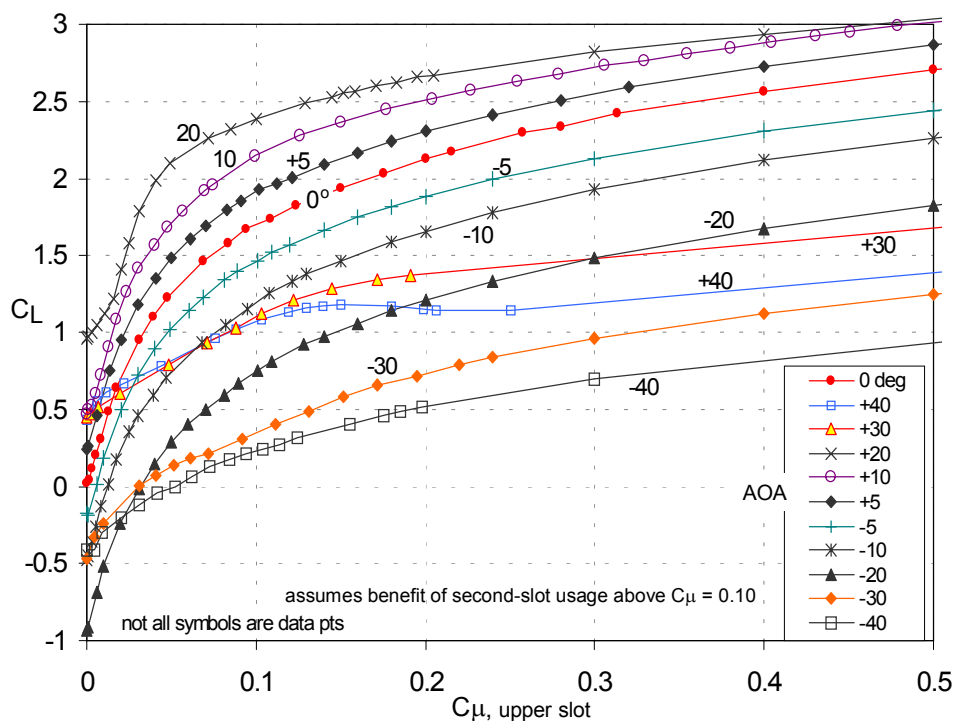Lift augmentation at +30 and +40 deg is low because leading edge separation has occurred before

Figure 28. Performance map for the pitch angles tested, with some curves extrapolated to higher $C\mu$ (not all symbols are actual data points). Peak demonstrated C_L is 3.0, more than double conventional capability.
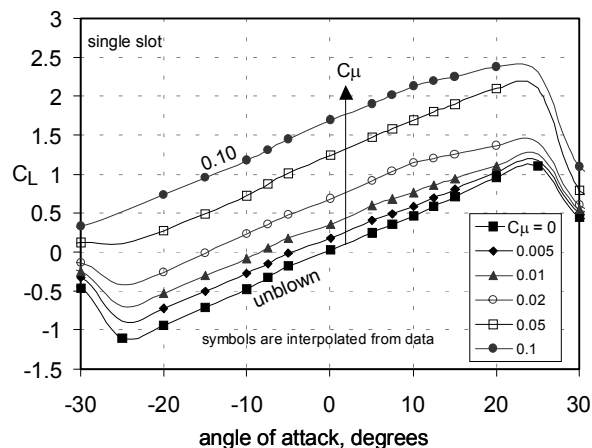
Figure 29. *Data of Figure 28 cross-plotted for constant Cμ (symbols are not data points). Leading edge stall sets the boundaries of efficient development of augmented lift.*

blowing was applied; the wing is in deep stall. In order to examine the performance implications of a three-dimensional flow field, elementary lifting line theory will continue to be used to provide perspective; it is recognized that the hydrofoil is not expected to have had a uniform chordwise or spanwise downwash velocity. On an airfoil, leading edge stall cannot be readily reversed by increased blowing. However on a wing, the downwash velocity can conceivably shift the equivalent two-dimensional AOA to a value below that where separation occurs. For example, at a wing pitch angle of 40 deg, an airfoil lift coefficient of 4 or higher (Fig. 9) should be obtainable if the wing could be made to operate at the corresponding airfoil condition of zero degrees while at a Cμ of 0.20. At a C_L of 4, the induced angle would equal the geometric setting thereby producing an effective angle of zero deg and attaining a viable operating condition, similar to that depicted in Figure 3. (This process could be envisioned as another load line in Figure 9 that started at +40 deg and went to a C_L of 4.0 at $\alpha_e = 0$.) This extreme state of circulatory lift, however, cannot ordinarily be achieved on the low aspect ratio wing because in the presence of extensive leading edge separation when unblown, the lift augmentation required to sufficiently shift the effective angle of attack cannot be produced. Conceptually, if the blowing were applied at a low pitch angle and then the model rotated to 40 deg, the desired state would exist (a path dependent process). The potential for hysteresis effects precludes this state from being operationally viable.

For the post-stall negative angles of −30 and −40 deg, the flow separation is on the side opposite the active slot. Somewhat better initial lift augmentation is achieved because flow is attached up to the slot, however, this time the downwash direction is such that

the leading edge separation is not alleviated. Thus there is an unavoidable penalty of being outside of the wing incidence range (+ or −26.5 deg) for which there is leading edge separation when unblown. Near the lower edge of that band at −20 deg, a C_L of 1.0 was produced experimentally. The maximum lift coefficient at a pitch angle of −20 deg is projected to be 1.8, when Cμ= 0.50. The estimated mean effective AOA of the wing section would then be −37 deg, which is considered viable based on the results of wind tunnel tests of CC airfoils at extreme angles. Higher coefficients of lift are available if a jet-flap mode of operation could be entered.

With the unblown stall angle establishing the pitch angle boundaries of high efficiency CC operation, future designs should consider increasing the leading edge radius beyond that corresponding to an ellipse.

Dual-Slot Jet-Flap Mode and Performance Projections

Limitations with respect to minimum tunnel speed and sizing of the slot pump precluded evaluating the hydrofoil at Cμ's above about 0.50, which is entering into the realm of the jet-flap. In addition, there would eventually arise limits due to the high-lift C_L's causing excessive jet/wake blockage and impingement on the tunnel floor, a model to test section size issue. To project performance into the high Cμ range associated with the dual-jet jet-flap concept, data and insight gathered from NACA investigations of jet-flap wings were used.[18,19] A NACA test model (Fig. 30) had strong similarities to the hydrofoil configuration, even though it had only one slot. The model used contouring on a rounded trailing edge to force lower surface detachment of the jet emitted from an upper surface
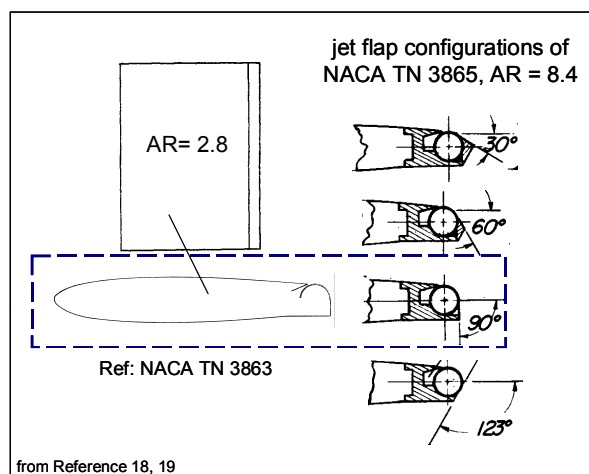

Figure 30. *NACA jet flap models with a tangential jet and forced detachment angle have similarities to current CC model when using second-slot counter-flow.*

tangential slot. (This design is something of a hybrid Coanda-jet-flap, but neither the slot location nor the ejection angle was appropriate for an efficient CC device.) It will be considered that the jet-flap configuration of Reference 18 corresponds to the hydrofoil when there is a flow from the secondary slot directed to controlling the detachment point of the primary jet. Supporting this viewpoint is that the NACA model jet ejection trajectory was 86 deg statically, the same as could be produced on the hydrofoil using 18% relative momentum flux from the second slot. Additionally, there is confirmation of the potential of the basic jet-flap mode of operation from the Variable Deflection Thruster concept of References 12 and 13, which is also based on combining two flows to produce a jet-flap. These perspectives, along with the simple behavior of jet-flap lift, permits a projection of dual-slotted CC performance to momentum coefficient levels well beyond those tested at the LCC.

Because of the significance to operational applications of being able to transition a CC device into a controllable jet-flap mode, some detail will be given of the procedures used to predict performance in that regime. Figure 31 is plotted in a manner analogous to the plots in the jet-flap study of References 18 and 19. Here it is assumed that at high $C\mu$ a part of the lift is derived from jet reaction force. A plot of $(C_L–C\mu)$ reveals the true circulatory lift increment ($C_{L\Gamma}$). To be observed in Figure 31 is that circulatory lift has almost leveled off at $C\mu=0.5$, while the overall lift continues to increment at a gain of 1.0. That is exactly the behavior of a jet-flap (except its relative inefficiency means a much higher $C\mu$ is needed to reach the circulatory lift limit). The procedure for synthesizing the hydrofoil performance curve is to identify for each AOA the $C\mu$ at which the local slope of C_L versus $C\mu$ becomes 1.0, that
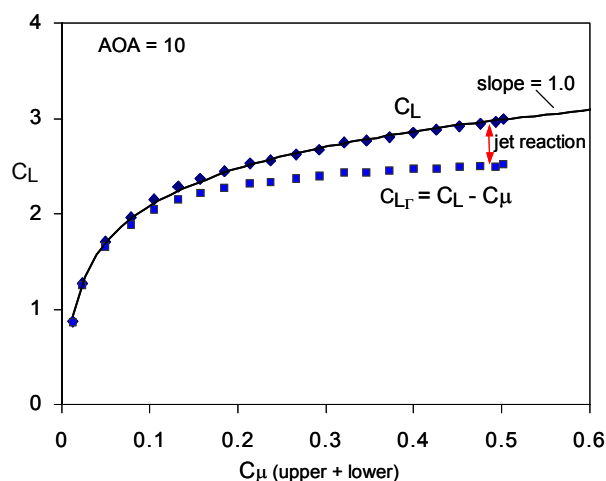

Figure 31. Subtraction of jet reaction force (Cμ) reveals the onset of circulatory lift limit at Cμ = 0.5.

is, the end of circulatory lift gain. This identification process can be accomplished with high confidence because of the linear trend that results when viewing the test data on a log scale plot as exemplified by Figure 27; a log curve-fit ensured consistency of the procedure. For $C\mu$ beyond the circulatory limit value (usually between 0.50 and 0.60), the C_L is allowed to increment only by the amount of jet reaction force, $C\mu$. Thus under the assumption of continued jet momentum force but no additional circulatory lift increment, the C_L performance curve can be projected all the way to $C\mu$'s corresponding to near-zero vehicle speed. Of course, this is stating that as speed declines, the available wing 'lift' becomes increasingly dominated by jet reaction force and the continued use of C_L to characterize performance becomes more of an accounting procedure.

While this water tunnel test could not cover all possible flow rates that might be encountered with a dual slot configuration, there does not, however, appear to be any upper limit to the momentum coefficient that can produce an increment in lift, since increasing the flow from the secondary slot should permit a transition into a merged dual-flow jet-flap mode of operation and with it the continued development of control surface forces for use down to extremely low vehicle speeds. Numerical values will be presented in a later section.

<u>Slot Flow Fence (Tip End Plate)</u>

Because of both the aft location of the tip vortex origin and the slot termination effects, a slot flow fence in the form of a small end-plate (Fig. 25) was briefly evaluated. An increment in lift was obtained and there were also benefits for the tip vortex cavitation properties. While the lift increased, the drag did not, and additional analysis showed an outboard movement of the center of lift; both are indications of reduced 3D effects. At the only other AOA, 20 deg, for which the plate was evaluated, the resulting lift increment was less. A larger tip plate of a more traditional size and shape was not evaluated, nor that of a much smaller plate directed to just edging the Coanda surface. There is the potential for significant benefits from the use of tip plates and the topic deserves additional consideration. They are currently in use on some conventional appendages. The use of surface flow visualization is recommended in conjunction with any future investigations.

<u>Pitching Moment and Centers of Loading</u>

By definition, the aerodynamic center (AC) is the chordwise location about which the pitching moment is not influenced by changes in lift. There are two such centers on a CC airfoil because lift can be developed in two independent ways, each having its

own moment center. On a wing, augmented lift causes an interaction between the load at the two AC's, resulting in a relocation of one of these centers versus that of the airfoil. The interaction is a consequence of the lift from CC, which is centered about midchord but which in turn causes a negative lift increment centered at ¼ chord due to the trailing vortices. Effectively, a moment couple is created making for an appreciable nose-down moment response when blowing is increased.

From a theoretical view, circulation control is equivalent to a conventional wing having a vanishingly small flap at the trailing edge. Reference 20 uses Lawrence's theory for thin rectangular wings of low aspect ratio to examine the implications of varying the flap chord length. In the case of a flap chord approaching zero length, the center of lift due to flap deflection is at 50%c for the infinite wing, as is the well-known finding for a CC airfoil. In contrast, for a short span wing of AR=2, the same theory indicates that the AC will be at 69%c, due to the effects of the induced angle of attack. Conversely, for a full chord flap—meaning a plain wing undergoing an AOA change—the AC is at 20.9%.

The experimental pitching moment (C_m) for the hydrofoil as resolved around the center of the root is presented in Figure 32; reference length is the mean chord of 24 inches. The plot shows the influence of operating at either constant pitch angle or constant $C\mu$. For a given C_L, a wide variation of C_m occurs, depending on the combination of incidence and blowing coefficient. Taking the slopes of these contour lines will reveal the two aerodynamic centers. Since it was found that the rolling moment corresponds to lift being
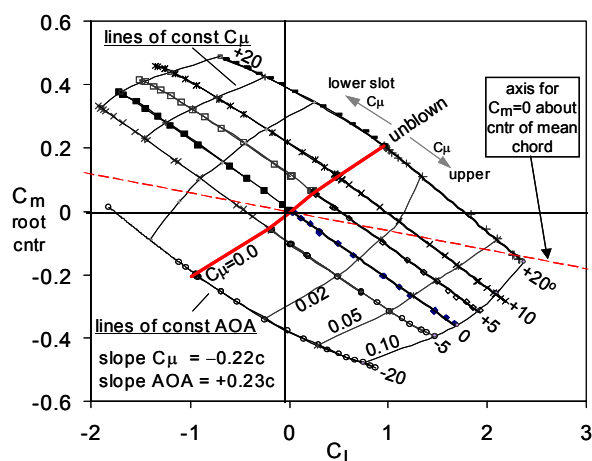

Figure 33. Two aerodynamic centers, for lift-due-to-pitch and lift-due-to-blowing. (Illustrative upper surface pressure computation is for C_L = 1.35, AOA = 12 deg. VSAERO)

centered at the 47% span location (both blown and unblown), the chord at that location will be taken as the mean chord for specification of the AC. For lift due to blowing, the AC is at 66%c, and for lift due to pitch angle it is 21%c (varies somewhat with $C\mu$ level). These locations are depicted in Figure 33 and are consistent with the findings and analysis made for the circular planform CC wing of Reference 14.

Figure 33 includes the upper surface C_p distribution from a VSAERO computation to illustrate operation at an angle of incidence. Leading edge loading has developed in response to the pitch angle of 12 deg, in accordance with the AC being at 21%c. There will be combinations of $C\mu$ and AOA where the load distribution becomes symmetric about mid-chord. These conditions can be determined by inspecting the pitching moment map of Figure 32 for points where the C_m is near zero. As a refinement, since the pitching moment was resolved about mid-chord of the root rather than of the mean chord, an offset adjustment can be made to allow placing a line on Figure 32 to represent zero moment about the model mean center. This new axis for $C_m=0$ has a special significance because the fore/aft symmetric chord loading provides an indication of when the wing effective angle of attack is zero, in keeping with elementary wing theory and CC properties. Where the special line for $C_m=0$ crosses the lines of constant pitch angle, the induced angle-of-attack as a function of C_L is indicated (it is very close to lifting line theory, not shown). This observation regarding $C_m=0$ was first made on the AR=1.27 wing of Reference 14 when it was subsequently evaluated over a large AOA range (unpublished). That model had pressure taps that permitted the confirmation of approximate fore/aft load symmetry when the C_m about the 50% chord was near zero. For the hydrofoil, panel method solutions provided confirmation.

Figure 32. Pitching moment (C_m) map formed by lines of constant pitch angle and constant slot momentum coefficient. Reference center is root mid-chord, the dashed line is for $C_m=0$ around the center of the mean chord.
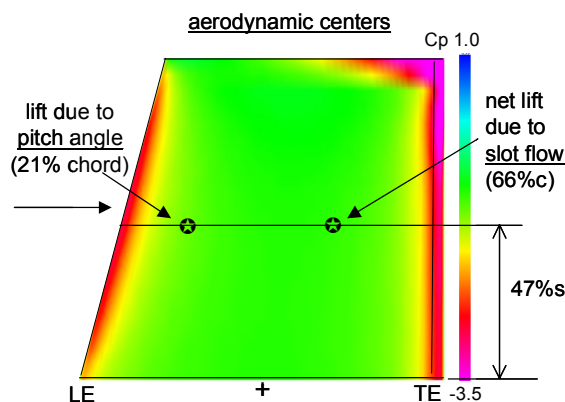
There is also a significance to the $C_L=0$ line. Potential flow solutions for a pure elliptical profile disclose that under these conditions the pressure distribution on the forward half-chord is an inverted reflection of the aft distribution, making the leading edge pressure peak similar to that of the trailing edge, except on opposite surfaces and in opposite direction of gradient. There is no surface pressure differential at mid-chord in that case.

The drag center (yaw_moment/drag at AOA=0) is found to be in the range of 46% to 50% span, depending on which data set is examined, essentially the same as for the lift center.

It is concluded that pitching moment loads developed on a CC wing are understood and accountable, although the current data set has not been examined to see if loads at extreme conditions of separated flow would exceed those which occur within the normal, predictable, range.

Mid-Surface Pressure Differential

Based on exploratory inviscid calculations, the mid-surface exterior pressure differential is a unique and linear indicator of total lift developed by the surface, independent of the source of lift. (More precisely, over a pitch angle range the Cp differential is a linear function of the normal force, C_N, rather than C_L.) That is true any time the pressure distribution is tracking that of a potential flow solution, that is, no significant flow separation. Monitoring and comparing this value of the pressure differential to C_L has long been a part of CC airfoil tests and is of value. Thus the hydrofoil was equipped with two centered surface taps to: 1) confirm any questionable trends from the load cell readings, 2) examine the feasibility as a source of a feedback signal for automatic load control, and 3) identify those operating conditions where a deviation in the pressure loading distribution developed.

Figure 34 is a collection of test data below a Cμ of 0.12, including various combinations of AOA, blowing level, and which slot is active. (The Cμ limit was selected to allow the use of all of the single slot data without the influence of the hypothesized excessive jet turning condition.) The linearity of the bulk of the data is striking, and even more so if plotted against normal force rather than lift. All AOA's between + and −10 deg coalesce. The relationship is that

$$C_L \sim 1.42 * \Delta Cp \qquad (5)$$

The factor of 1.42 compares to 1.50 determined from the VSAERO panel code.

It is concluded that the mid-surface pressure differential can be used as an operational indicator of
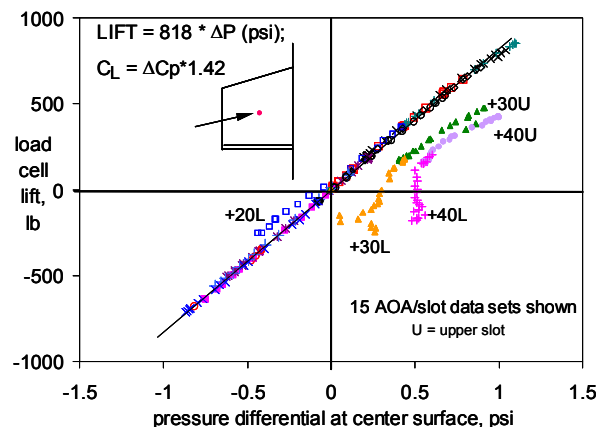

Figure 34. Mid-Surface pressure differential linearly correlates with lift loading for attached flow conditions; reveals those conditions that result in flow separation. (Similar result if viewing normal force.)

appendage control force, just as proposed for use on helicopter blades[13] and confirmed on a high aspect ratio wing in Reference 21.

It is readily apparent in Figure 34 when adverse flow conditions begin to develop at extreme conditions. The offset of the 30 and 40 deg data is a consequence of the flow separation when beyond the angle of unblown stall. The 20 deg data shows deviation at higher blowing levels just as the zero-lift line is crossed. Examination of pressure distributions as predicted by a panel method did not disclose any expectation of separation; the 20 deg result is unexplained.

CAVITATION

Cavitation will occur when the minimum pressure reaches the value corresponding to vaporization of water, about 0.5 psia, depending on temperature. The cavitation index, σ, is the term for the absolute value of the pressure coefficient (–Cp) that will result in vaporization and is a function of test section static and dynamic pressure. In general, minimum pressure (Cp_{min}) on a CC lifting surface occurs downstream of the slot, usually about halfway to the end-of-chord, depending on the incremental C_L. The value of Cp_{min} is a result of the geometry and the degree of circulatory lift. There is also an additional contribution to Cp from the pressure differential across the curved wall jet, given by

$$\Delta Cp = -C\mu/(r/c); \quad r/c = 0.043 \qquad (6)$$

Something of an unknown, however, is the pressure field in the region of the slot nozzle lip edge. This is where the upstream flow is initially entrained, and

20

where there is the effect of the lip face, which on this model was square-cut with a thickness of about one-third of the exit opening. Thus, there is the possibility that Cp_{min} exists at the slot exit. One of the research objectives was to determine where Cp_{min} occurs and what the impact of subsequent cavitation would be on the ability of the jet to induce circulatory lift, or even to remain attached.

To investigate cavitation on the model, rather than increasing tunnel speed (a model loads concern), test section static pressure was reduced from the nominal value of 25 psia to about 10 psia. The slot flow from the hydrofoil was then gradually increased while under observation for evidence of cavitation, disregarding the tip vortex. Random localized flashes of cavitation began over the Coanda surface, presumably due to vortical structures within the jet. As slot flow continued to be increased, cavitation abruptly enveloped the full extent of the wall jet, wrapping around the end-of-chord (Fig. 35). The origin of the cavitation sheet was the slot lip face, as judged by the edge-wise observation made possible due to the LDV viewing window. Underneath this sheet emanating from the lip, there appeared to be un-cavitated flow. The non-uniform spanwise distribution seen in Figure 35(a) is because this is right at cavitation inception and, most likely, minute differences in lip finishing or gap settings result in an uneven onset. The value of σ implies that the local pressure coefficient at the slot for the first appearance of sustained cavitation is –6.6 for a C_L of 1.02, which is useful for future CFD development and for projection of compressibility effects in aeronautical applications.

As the duct pressure was increased even further, lift continued to rise, with the spanwise extent of jet cavitation becoming uniform, Figure 35(b). Eventually the lift began to roll over, as depicted in Figure 36. At no time did the Coanda jet detach prematurely from the trailing edge, as had been a concern because of previous experience with compressible flow when shock waves developed. It is not known how nozzle lip thickness or contouring affected these results. It may even be that having a lip design that cavitates first will inhibit the circulation enough to preclude the wall jet from reaching an internal pressure corresponding to σ.

Attempts to initiate cavitation at other than the trailing edge by pitching the model were not successful because the nature of the 3D flow field largely precludes obtaining Cp_{min} upstream of the trailing edge under high lift conditions.

The wind tunnel test report for the parent airfoil section contains a plot of measured Cp_{min} as a function of lift coefficient and angle of attack, which can be used for cavitation assessments.[7] The data indicates that a Cp_{min} of –6.6 at a C_L of 1.0 would occur at an effective AOA of –9 deg. This is very close to the
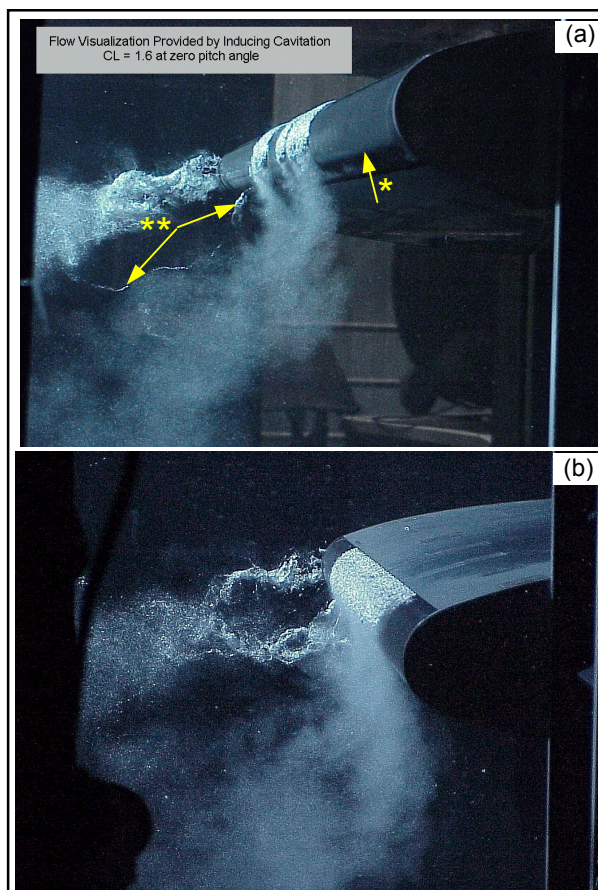
*Figure 35. (a) Static pressure of tunnel reduced until occurrence of first surface cavitation; (b) with continued increase in slot flow. *(Shadow line; lighting angle is from above, shadow zone gives false indication of inner edge of the turned flow.) **Vortex emanating from ~80% span.*
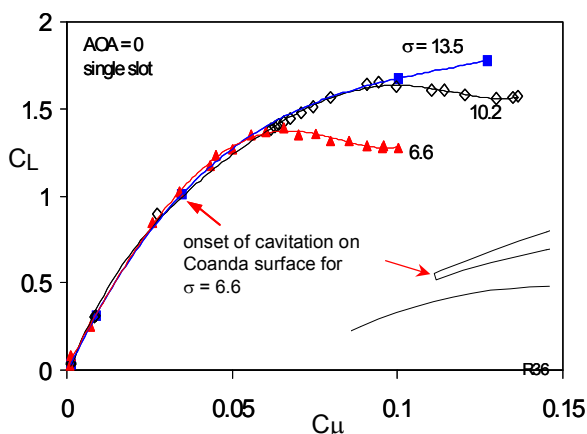
Figure 36. Lift response to cavitation development on the Coanda surface: eventual soft roll-over.

estimated induced AOA on the hydrofoil at the onset of cavitation. However, that match assumes that a true 2D equivalent condition prevails on the lifting surface, a chordwise downwash uniformity question. The Cp_{min} from potential flow solutions was also examined, but found to be inadequate as an indicator of cavitation onset. This is seen in Figure 4 where the Cp_{min} happens to be the -6.6 of interest, however, the C_L is 1.5, not the 1.0 found in the LCC test. This under prediction of negative pressure in the Coanda region is an expected result of having to fair over the slot gap discontinuity to enable inviscid computations. If an increment in the trailing edge region pressure due to the momentum of the jet ($\Delta Cp= -1.6$, Eqn. 6) is added to the calculated Cp a somewhat closer agreement with the experiment would be obtained; also observed in Figure 3.

Cavitation provided a flow visualization opportunity (Fig. 35). Note, however, that the lighting angle for the photographs cast the underside of the model into a dark shadow, giving a false indication of the inner edge of the flow that has wrapped around the end-of-chord. Most unfortunately, the underside region of the hydrofoil where the influence of second-slot discharge would be seen was in this photographic shadow zone. Visual observation at the time revealed local flow field changes with just the slightest slot outflow.

Reduction of tunnel static pressure resulted in vortex core cavitation well before occurrence of any surface cavitation. A number of vortical structures in the flow field were thus revealed, some of a transient nature. Of interest for future CFD analysis was a weak but sharply defined and persistent secondary vortex at about the 80% span position that seemed to emanate perpendicularly from the rounded trailing edge, near the lower surface slot. This curious secondary vortex became wrapped up in the tip vortex, visible in Figure 35. Video recordings were made as part of these investigations.

In terms of the practical implications of these findings, the conditions of speed and pressure depth corresponding to trailing edge cavitation are outside of the proposed operating regime on an underwater vehicle. Moreover, even if cavitation does occur in certain circumstances, the impact is a benign reduction in blowing effectiveness, as opposed to a buffeting or abrupt lift stall. Even though the overall effects are benign, the tip vortex cavitation was strong. The flat wing tip cap, combined with no spanwise variation of the slot gap for load tapering, made for early cavitation of the tip vortex. The trial of the small tip end-plate, discussed previously, showed that changes in tip cap geometry would alleviate the tip vortex.

DRAG CHARACTERISTICS

The unblown drag coefficient (C_{D_O}) is 0.0186 at zero pitch angle, which is consistent with 2D CC tests and about twice that of a conventional profile with the usual sharp trailing edge. For low aspect ratio lifting surfaces, lift-induced drag quickly becomes the dominant drag component as control forces are developed. Figures 4 and 5 show how the lift-associated drag develops at zero AOA in a potential flow solution. The negative pressure in the trailing edge region does not have an offset at the leading edge, due to the effect of the wing downwash on the front stagnation point location. For the present discussion of test results, induced drag, C_{Di}, will be the term applied to all the drag changes that are associated with the development of lift and will inherently include such effects as variation in frictional drag, slot thrust recovery, and separated flow effects.

Because theoretical drag tracks lift so directly, drag data is presented not as a function of $C\mu$, but rather in relation to C_L. A CC wing can develop a range of lift coefficients at any given fixed pitch angle. By switching from one slot to the other, the lift can be incremented or decremented from the unblown value, including passing through zero lift. Thus there is a wide drag polar diagram for each pitch angle. In Figure 37 the test data is arranged as if it all corresponded to the model being set to a positive AOA with the full control range being obtained by switching the upper/lower blowing slots. In the range of 0 to +20 deg for upper slot operation, the drag is essentially a function of lift without dependence on the source. For example, the unblown drag for 20 deg equals that at AOA=0 with the same lift obtained by blowing. At higher angles were there is flow separation, there is a displacement.

Figure 37 presents the drag trends for up to moderate blowing levels ($C\mu< 0.12$). For each AOA
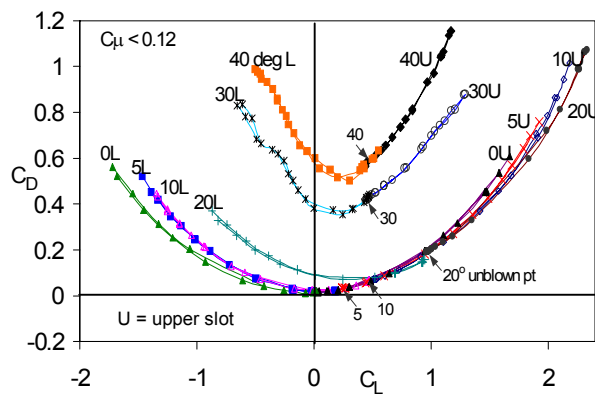

Figure 37. Drag polars depicted at fixed pitch angles by combining data from upper and lower slot modes.

there is a drag minimum near but not exactly at C_L=0, that is, there is an offset from C_L=0. This pattern is analogous to that found for aircraft with deflected flaps. If the C_L is now both shifted to counter this offset ($C_L-C_{L_{min}}$) and squared to produce a parabolic polar diagram, the drag data collapses to form several nearly straight lines, one of which captures all AOA's below 10 deg (not shown). The slope of these lines can be used to identify the Oswald wing lifting efficiency factor (e), for use with the familiar induced drag equation from Prandtl's wing theory (Eqn. 7). The value for e ranges from 0.80 for those AOA's below unblown stall to 0.20 at 40 deg.

$$CD_i = CD - CD_{min} = (C_L - C_{L_{min}})^2 / \pi ARe \qquad (7)$$

In a complete numerical modeling of drag, CD_{min}, $C_{L_{min}}$, and e are empirical functions of AOA.

When unblown, the span efficiency factor e was found to be 0.83, not unlike that of a conventional rectangular wing (Whicker's data shows 0.88 for an appendage with a 0.45 taper ratio). It can be concluded that induced drag for lift developed by CC (e=0.80) is essentially the same as that from conventional sources of lift. This is likely a result of the spanwise $C\mu$ being nearly constant on the model configuration as tested, making the augmented load distribution close to that from incidence. A design optimized for a particular application might not have a constant spanwise $C\mu$, for reasons of tip vortex strength or reduction of slot mass flow or of induced drag reduction.

WAKE FILLING, THRUST RECOVERY, LDV

LDV surveys were made to determine the ability of dual equal slot flow (no lift) to eliminate the wake momentum deficit that results from drag. This is a desirable goal if there are downstream devices, such as propellers, that would be adversely affected by a non-uniform flow field. Referred to as wake filling, or momentumless wakes in Reference 22, the concept is that at some operationally relevant point downstream the jet momentum will have been sufficiently transferred to the remnants of the surface boundary layer flow to make the wake momentum profile uniform with that of the locally prevailing flow.

Using LDV rather than a pressure probe array to survey the wake profile requires a large investment in time, hence it was not practical to iterate on identifying the slot flow setting that exactly eliminated the wake deficit. It was decided to use a setting that gave a zero drag force, although it is recognized that theoretically a deficit-free wake does not correspond to a zero drag reading on the model balance. A true filled wake

requires that $CD = -C\mu * V_\infty / V_{jet}$, a paradox of model drag and wake momentum deficit that is a result of the slot flow originating from outside of the test section, rather than from an intake on the model itself; see the brief explanation by Kind in Reference 8.

Wake sighting locations for the LDV were limited to the near-region (0.02 to 0.27c) which is well before complete jet mixing, and to rather far downstream (2.2c), which may be beyond operational interest. Park's studies[22] of a somewhat related dual jet laboratory model showed that the required distance was about 4 chord lengths for a near-flat profile to emerge. However, there are questions of Reynolds number and the relevance of Park's flat base configuration to the present geometry. On the hydrofoil model, the dual jets could merge on the rounded surface and depart into the wake as a single central jet. The closest survey plane, for V_{jet}/V_∞ = 2.8 and downstream by about ¼ of the
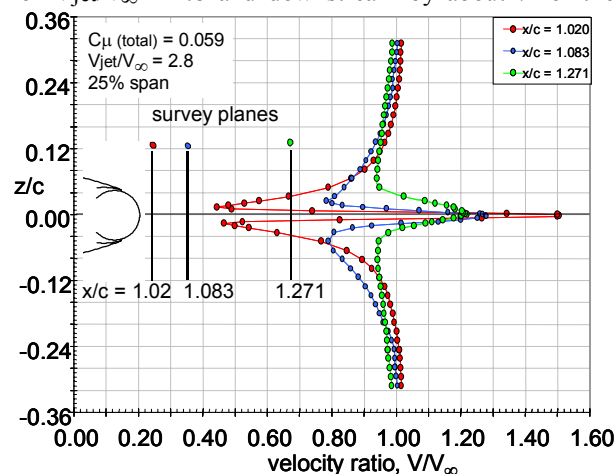

Figure 38(a). Near-field wake profile at three locations for equal slot flow rates. Portrayed geometry is scaled to the y-axis.
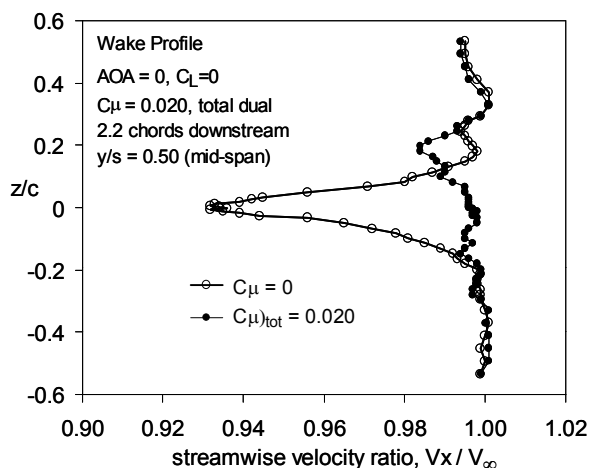

Figure 38(b). Wake filling. Velocity profile two chord-lengths downstream, for dual slot $C\mu = C_D$.

Coanda diameter D, showed a single sharply defined jet of width 0.27D that penetrated the center of the wake, Figure 38(a). As expected, the jet width rapidly increased downstream as peak velocity decayed.

A velocity ratio of V_{jet}/V_∞ =1.6 was found to produce a load cell reading of zero drag. Figure 38(b) illustrates the wake filling result, for mid-span at a location of 2.2 chord lengths from the trailing edge. The wake profile has been favorably influenced by the momentum flux from the two slots. The profile inflection just above the original wake location is from unknown sources, but at a distance of 2 wing spans, other flow field structures from the tip or root may have entered the survey plane. Identification of the minimum downstream distance required for adequate development of uniformity will require additional experiments where greater access is provided along the wake path for the survey instrumentation. No examination was made for evidence of Karman vortex shedding interaction with the dual jets, as reported by Park on a flat-base configuration.[22]

The zero drag condition established for the wake survey permits an assessment of slot thrust recovery at low blowing. Two opposing factors are involved in slot propulsive efficiency: increased drag due to jet entrainment reducing local pressure on the aft facing surface, and drag reduction by delay of separation on the upper and lower surfaces. A condition of minimum power might result from the net influence of these effects at which point there would be some

value to having a continuous flow from the slots in cruise. The condition that produces zero drag is at a Cµ of 0.0194, which corresponds to a propulsive thrust recovery of 96% for this configuration, where the total slot exit area is 0.38% of planform surface area. That compares to the typical 90% found with CC airfoils when drag is based on corrected wake rake readings. The 96% is higher than both that found statically (80%) and that reported by AMO Smith[15] (80%), although his data is largely for much higher Cµ's. Data for the hydrofoil with both slots equally active is not extensive enough to make a general statement on propulsive efficiency, if this mode of operation is of interest.

Figure 39 is presented to illustrate the general nature of the flow field in the trailing edge region while at moderate levels of lift augmentation. This LDV data was acquired to support future CFD validation efforts. The C_L of 1.4 is somewhat less than that corresponding to the inviscid solutions presented in Figures 4 to 6 (C_L=1.5). Figure 39 was selected to show the unsteady component of vertical velocity, to better disclose the location of the (turbulent) jet and wake. The trajectory change toward the tip likely results from the non-elliptic load distribution. Both the tip and root region planes show a vortex in the field. The root vortex would be arising from the root-wall juncture, which was without any special treatment to control the splitter-plate boundary layer; there is also a ¼ inch cover plate at the root and a wall gap. The trailing edge close-up photograph in Figure 13 shows the root-wall geometry
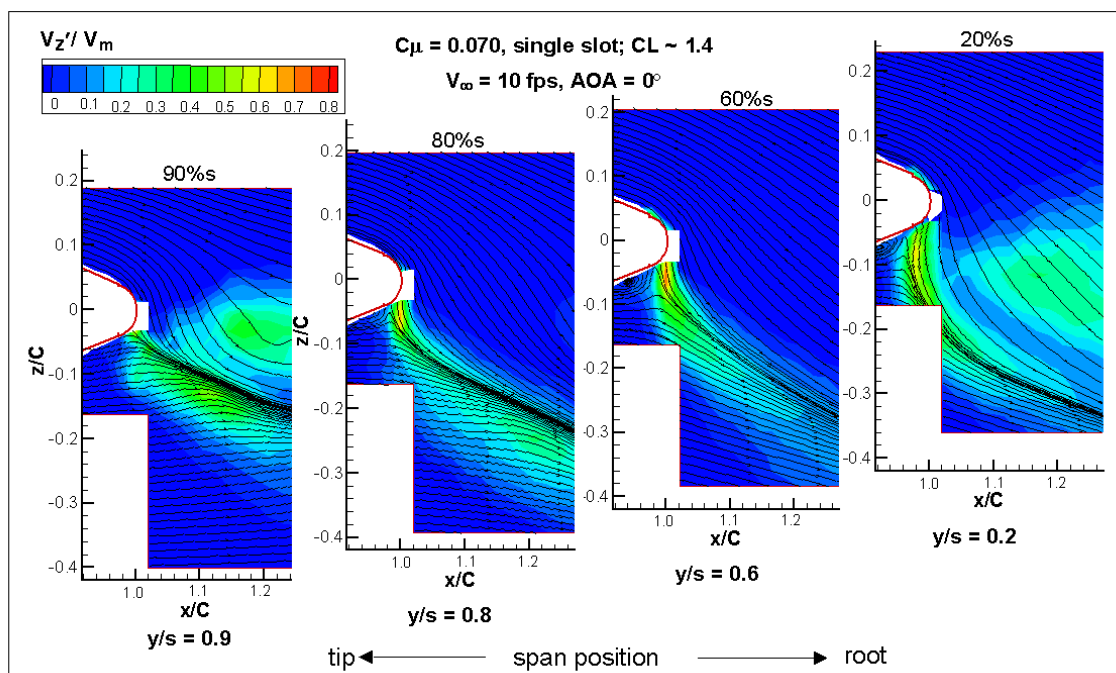

Figure 39. LDV flow field survey at four span positions, showing the turbulence in the vertical direction to reveal the location of the jet and wake.

and also happens to indicate the jet trajectory at the slot termination: the light colored region which may be discernable on the lower surface next to the plate is from the absence of the jet (no staining of the brass surface by the slot flow).

SUGGESTED FOLLOW-ON INVESTIGATIONS

Lifting Surface Theory

It was apparent from using lifting surface flow solutions (VSAERO) for the CC hydrofoil that the chordwise pressure gradients differed somewhat from that of any possible operating condition in two-dimensional flow (infinite wing). The chordwise load on the AR=2 planform is shifted away from mid-chord, as would be the effect of a negative camber. This is an expected consequence of an induced velocity that varies along the chord line, effectively making a large-chord wing operate in a curved flow field. The result is that the wing section profile undergoes a change in equivalent 2D geometry as lift is developed. Whereas the airfoil contour used on the hydrofoil is reasonably tolerant of these changes in pressure gradients, there needs to be an awareness when airfoil designs are undertaken in the future, especially for any wing aspect ratios lower than that on the current model. Therefore, it would be helpful to have an analytical extension of lifting surface theory that would quantify the impact of CC-like chordwise loads on the corresponding changes in equivalent camber and/or thickness ratio of a wing. Analogous developments for wide-chord marine propeller blades are available in the literature.[27]

Experimental

In addition to using the recently acquired data to validate a viscous flow CFD capability to guide future designs of the trailing edge details, this is a summary of how the investigation described in this paper could be supplemented with additional experimental work (None of the following is a prerequisite to an at-sea demonstration, depending on program objectives.)

There is at least one report in the literature of instabilities in the location of the merger of two wall jets on a convex surface. Because disturbances in the trailing edge can manifest as oscillations in foil loading (via the concept of Theodorsen's oscillating flap analogy), unsteady pressure sensors are needed upstream of the slot, perhaps at model center.

It is anticipated that inviscid panel-method solutions will be the primary design tool for examining planform load distributions. To confirm the chordwise pressure gradients predicted by a panel code, a complete circumferential row of pressure taps should be placed at mid-span. To monitor span load and trailing edge pressure conditions, surface pressure taps are also recommended in at least three spanwise stations at mid-chord, at the end of chord, and inside the duct.

A LDV would be useful in studying the influence of lower slot ejection, as well as operations in the dual-jet jet-flap mode. Water dyes from the slots could help in confirming that the fluid dynamics is correctly understood. Cavitation as a flow visualization technique should be exploited, with special attention given to the odd vortex structures in the outboard trailing edge region that are so clearly revealed when the cores cavitate.

For an extension of the cavitation studies, one of the slot nozzle lips could be beveled to form a near knife-edge. The objective is to determine if the nozzle edge continues to be the point of inception. There may be some performance and/or acoustic aspects associated with beveling. A tip cap design directed toward tip vortex core strength reduction is also recommended.

There are certain tests better suited to a wind tunnel. Those include wake filling surveys (real-time profiles presented via a wake rake), influence of slot gap settings, end-plate optimization, and surface flow visualization. Time required to gain access to the model is the key factor when configuration iterations are involved. In conjunction with the wake filling study, a search can be made for any drag minima that might provide a good degree of propulsive efficiency. The lift curve slope with both slots equally active should be examined. The rearward directed jet sheet may effectively act as an extension of the chord, if so, it provides a means of adjusting static stability.

If a proposed operational application is to depend on the jet-flap or static thrust vectoring modes, additional model scale tests need to be conducted. Simulation of operation at these low speeds requires a large size facility, in order to avoid wake/jet blockage effects. The data and insight are needed to both verify the high $C\mu$ projections made from the LCC results and to examine how creep-speeds would influence the available thrust vectoring angle. A test in a tow basin may be suitable, where a model would be mounted like a rudder. Astern operations could be evaluated at the same time. Potential for cavitation requires review before committing to an unpressurized test facility.

The hydroacoustics of CC operation was addressed only indirectly in the current investigation. Reference 24 shows that a key question is whether the slot flow as it exits is laminar (desired) or turbulent. Visual observation of water ejection into air showed that the jet sheet was clear for several slot gap lengths before becoming white. This was taken to indicate laminar flow, however, a nozzle flow experiment needs to be

performed at full scale Reynolds number with proper instrumentation for a definitive answer.

OPERATIONAL SCALE CONSIDERATIONS

As for the question of Reynolds number effects, there is no consensus that a Rn effect for lift-due-to-blowing has been identified, other than what occurs indirectly through Rn effects on the unblown characteristics on which the augmented lift is superimposed. In certain circumstances, those unblown properties can make a notable impact, as when a change in Rn causes a shift in the flow separation point upstream of the slot.

Of more significance when projecting CC results to a full scale application is what value of $C\mu$ to consider. The available $C\mu$ for a given pump power setting is a strong function of speed, covering orders of magnitude if one considers stopping or extreme maneuvering conditions, Eqn 1. For hydrodynamic application, Figure 40 shows $C\mu$ as a function of speed and pump power loading (ideal horsepower per square foot of control surface). The relationship of slot momentum flux to pump power and flow volume is a function of slot gap setting, a factor that also influences the CC lift augmentation ratio. Slot gap effects were not addressed in the present investigation, but have been examined elsewhere, Reference 23 for example. A power loading of 1 is about what was available during the CC hydrofoil test and was chosen based on the desired parametric range at the nominal water tunnel speed. A value of 1 might also be recommended for initial consideration for a speed regime of 5 knots and below, since for most applications the requirement for augmented lift would be expected to taper off at higher speeds. The current test results have led to the belief that the extremely high momentum coefficients ($C\mu>1$) that are inherently available at low speed can be converted into viable control force increments by entering a dual-jet jet-flap mode of operation. There is no longer any reason to consider the need to restrict the pump output in accordance with speed to prevent excessive slot momentum coefficients.

Using the jet-flap analogy to project hydrofoil test results to conditions well beyond those that could be obtained in the LCC, Figure 41 shows the available coefficient of lift at zero pitch angle. Figure 42 presents on a log scale the corresponding dimensional forces produced by a representative CC control surface. Augmented force availability as a function of speed differs markedly from that of the conventional appendage, at 1 knot the available force is 10 times that of a conventional appendage. The two ends of the speed regime are characterized by non-dependence on
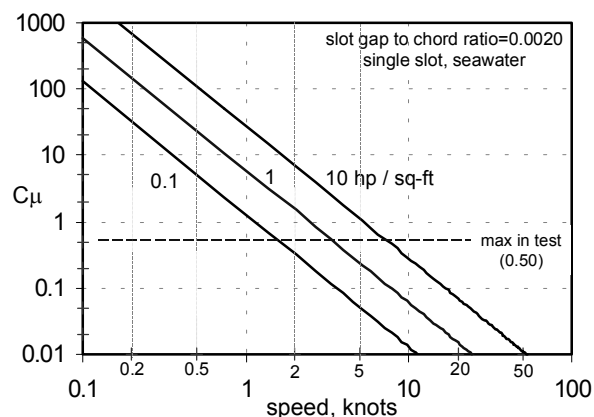

Figure 40. Available $C\mu$ as a function of speed and ideal pump power loading (hp/sq-ft).
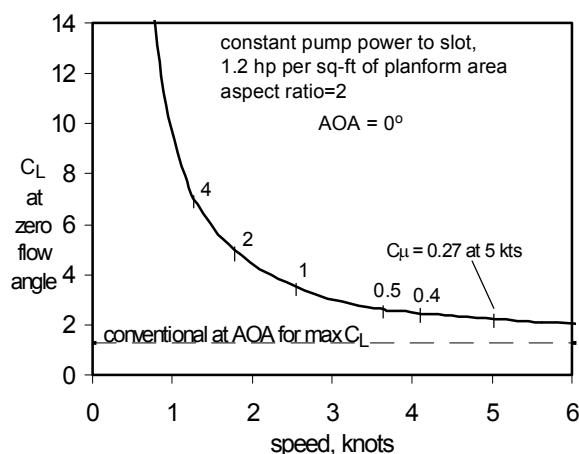

Figure 41. Projected lift coefficient of a CC appendage at a power loading of 1.2, without benefit of pitch angle.
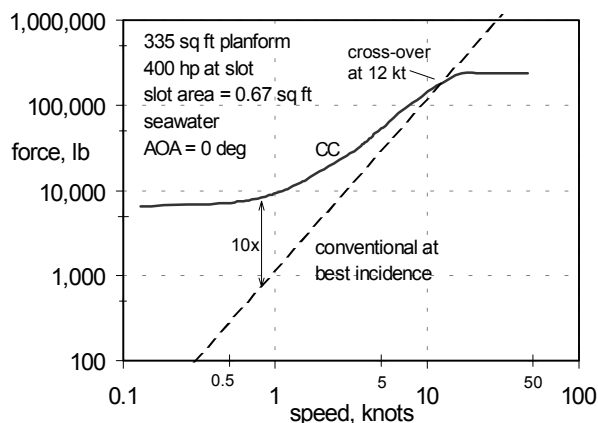

Figure 42. Control force capability (example) versus speed for same conditions as in Figure 41, dimensional units on a log scale. Additional force would arise with angle-of-attack.

speed. At the low speed end, the jet reaction force is the residual when other fluid dynamic forces have decayed. At high speed, the $C\mu$ has declined to where the C_L versus $C\mu$ relationship is linear; the result is that the lift due to blowing no longer has any dependence on velocity. The ratio of control force available at the two ends of the speed regime is simply the basic augmentation ratio of 36 as determined in the LCC test results (lift from pitch angle is additional). In the example of Figure 42, there is a crossover between the capability of a fixed-pitch CC appendage and the corresponding conventional surface at a certain speed. That speed could be used as a power loading sizing parameter.

A frequent question is what jet velocity ratios (V_{jet}/V_∞) are required for CC hydrodynamic applications. The answer is derived from Equation 1 where h/c is the slot gap to chord ratio. The value of h/c needs to be in the range of 0.0010 to 0.0030, going above that value would be acceptable only after a risk reduction experiment. The short answer to the velocity ratio question--other than it is situationally dependent-- is "up to 7 or more, although appreciable benefits are obtained with 3 or less". The slot gap on a full scale CC appendage would be about 3/8 inch, the optimum value would be determined in a system design parametric trade-off. Decreasing the gap reduces flow volume but increases the required pressure.

Application studies for submersible vessels would need to consider such matters as wing-body lift carryover and the applicability of conventional flow interference factors. Appendage-to-hull gaps and the potential for separation of the hull boundary layer are other effects that need to be modeled, but probably are of second-order concern.

A major question to be decided is if the CC appendage is to be fixed-pitch or moveable. The flow field environment in a maneuvering turn may make the rudder the probable surface to have to remain moveable, however, an operational analysis may show otherwise.

The current test has addressed steady state operation. It needs to be recalled that the forte of trailing edge blowing is to provide a means of easily and rapidly modulating the forces developed by the surface. The modulation of the slot flow has been demonstrated to null the effects of periodic flow field disturbances, as in Reference 25, and to control vibratory loading on rotary devices. Conversely, it has been used to generate unsteady disturbances for beneficial purposes[26]

The performance capability documented by this test applies only to a configuration using a full span slot. For a given control force requirement, substantial pumping power and induced drag penalties are involved with any form of part-span blowing, unless the intent is

to generate vortices for the purpose of a braking effect, which has been demonstrated on an annular wing by spatially alternating which spanwise slot is active.

SUMMARY OF FINDINGS AND CONCLUSION

Performance as a prospective control surface appendage on marine vehicles exceeded expectations, primarily because of the ways found to derive benefits from a dual-slotted configuration.

Based on the test results of this CC wing of effective aspect ratio 2, the following observations are made:

- Circulation control (CC) applied to low aspect ratio wings is just as effective as on high aspect ratio surfaces, relative to basic finite wing theory. The significance is that no penalties of a short wing span were found that are unique to development of lift by a slotted Coanda-effect trailing edge.

- Positive lift is obtainable even at a geometric pitch angle of minus 40 degrees, the most extreme angle evaluated. The highest demonstrated lift coefficient within the limits of the test setup met expectations and was 3.0, more than double that of a conventional ship appendage of the same planform. Maximum circulatory lift coefficient (subtracting the presumed jet reaction force) was 2.5.

- Angle-of-attack range for efficient lift augmentation is essentially set by the unblown stall angle

- General performance trends are readily predictable by using the graphical concept of a wing load line (induced angle of attack as function of lift) imposed on the performance map of the parent CC airfoil.

- Induced drag from augmented lift is as expected from a lifting surface, the Oswald span efficiency factor was about the same as when unblown.

- The location of the two chordwise aerodynamic centers of lift, as it relates to pitching moment, met expectations. Lift due to angle-of-attack is centered about the 21% chord while the center of net lift due to blowing is located at 66%. Spanwise (roll) center was found to be at 47% span.

- When cavitation was forced to occur on the Coanda surface at high lift levels, there was no abrupt stall, only an eventual soft roll-off of lift. Cavitation originated on the nozzle lip

face for the tested model and encompassed the wall jet to the end-of-chord, without premature jet detachment.

- The flat tip-cap design chosen for the wing model produced a tip vortex that cavitated earlier than on conventional hydrofoils. Cap contouring and span load distribution needs special attention due to the high lift and aft location of the vortex formation. A small end-plate in the aft region of the tip incremented lift and reduced vortex cavitation.

Dual slots have advantages other than providing for production of symmetrical control forces. Exploration of simultaneous operation of the second slot revealed benefits of significant operational implication:

- Substantial increases in the maximum lift increment available from single slot blowing are obtained by a small flow from the second slot, due, it is believed, to the prevention of excessive turning of the primary wall jet when beyond moderately high momentum coefficients.

- Increased second-slot flow forms a merger of the two wall jets into a directable planar free jet. One virtue is that a jet-flap mode of lift augmentation becomes available at the extreme blowing coefficients obtainable at low vehicle speed. This results in a continued increase in lift coefficient when the circulatory lift increment available from the basic CC effect asymptotes at high blowing. Thus a high efficiency CC design can be transitioned into a jet-flap mode for those operating regimes in which it is the most appropriate form of active flow control.

- A second virtue of dual slots is that a full 0-360 deg thrust vectoring mode is available for maneuvering forces at essentially zero speed, with a thrust recovery of 70-80%. There does not appear to be any limit to the momentum coefficient that can be converted into a usable control force, at any speed.

- The potential to produce a wake free of velocity deficits (wake filling) was confirmed by LDV survey. Identification of the minimum downstream distance required for adequate development of true uniformity will require additional experiments where greater access is provided along the wake path for the survey instrumentation.

LDV surveys for use in CFD validation were made of the aft flow field for two representative operating conditions.

Although there remains some technology topics that merit additional investigation, no reason was found to not proceed with a large scale operational evaluation of an appendage that incorporates the active flow control technology described herein.

REFERENCES

1. Newman, B. G., "The Deflection of Plane Jets by Adjacent Boundaries – Coanda Effect," in Boundary Layer and Flow Control, Vol. 1, G. Lachmann, ed., Pergamon Press, 1961, pp 232-264.

2. Willie, R., and Fernholz, H. "Report of the First European Mechanics Colloquium on the Coanda Effect," J. Fluid Mechanics, Vol. 23, part 4, 1965, pp. 801-819.

3. Englar, R. J., "Circulation Control Pneumatic Aerodynamics: Blown Force and Moment Augmentation and Modification; Past, Present & Future," AIAA Paper 2000-2541, June 2000.

4. Englar, R. J., and Applegate C. A., "Circulation Control – A Bibliography of DTNSDRC Research and Selected Outside References (Jan 1969 – Dec 1983)," DTNSDRC, Report 84/052, Sept. 1984.

5. Davenport, F. J., "A Further Discussion of the Limiting Circulatory Lift of a Finite-Span Wing," J. of the Aerospace Sciences, Dec. 1960, pp. 959-960.

6. Helmbold, H. B., "Limitations of Circulation Lift," J. of the Aeronautical Sciences, Vol. 24, No. 3, Mar 1957, pp. 237-238.

7. Abramson, J., "Two-Dimensional Subsonic Wind Tunnel Evaluation of a 20-Percent-Thick Circulation Control Airfoil," DTNSRDC, ASED 311, June 1975.

8. Kind, R. J., and Maull, D. J., "An Experimental Investigation of a Low-Speed Circulation-Controlled

Airfoil," The Aeronautical Quarterly, Vol. 19, May 1968, pp. 170-182.

9. Englar, R. J., and Williams, R. M., "Design of a Circulation Control Stern Plane for Submarine Applications," NSRDC, TN AL-200, March 1971.

10. Etter, R. J., and Wilson, M. B., "The Large Cavitation Channel," Proc. 23rd ATTC Meeting, New Orleans, LA, June 1992.

11. Rew, H. S., and Park, S. O., "The Interaction of Two Opposing, Asymmetric Curved Wall Jets," Experiments in Fluids, Vol. 6, 1988, pp. 243-252.

12. Kizilos, A. P., "Fluid Flight Control Feasibility Study using the Variable Deflection Thruster," Honeywell Inc., 12016-FRI, AD378303, Dec. 1966.

13. Bailey, R. G., and Hammer, J. M., "Helicopter Application Studies of the Variable Deflection Thruster Jet Flap," Honeywell Inc., 12153-FR1(R), Nov. 1970.

14. Imber, R. D., and Rogers, E. O., "Investigation of a Circular Planform Wing with Tangential Fluid Ejection," AIAA Paper 96-0558, Jan. 1996.

15. Smith, A.M.O., and Thelander, J. A., "The Power Profile, A New Type of Airfoil," Douglas Aircraft Company, MDC J6236, Jan. 1974; also a summary in AIAA Paper 74-939.

16. Whicker, L. F., and Fehlner, L. F., "Free-Stream Characteristics of a Family of Low-Aspect-Ratio, All-Moveable Control Surfaces for Application to Ship Design," DTMB Report 933, May 1958.

17. Abramson, J., "Two-Dimensional Subsonic Wind Tunnel Evaluation of Two Related 15-Percent-Thick Circulation Control Airfoils," DTNSRDC, ASED-373, Sept. 1977.

18. Lowry, J. G., and Vogler, R. D., "Wind-Tunnel Investigation at Low Speeds to Determine the Effect of Aspect Ratio and End Plates on a Rectangular Wing

with Jet Flaps Deflected 85°," NACA, TN 3863, Dec. 1956.

19. Lockwood, V. E., et al., "Wind-Tunnel Investigation of Jet-Augmented Flaps on a Rectangular Wing to High Momentum Coefficients," NACA, TN 3865, Dec 1956.

20. Campbell, I. J., et al., "Aerodynamic Characteristics of Rectangular Wings of Small Aspect Ratio," ARC, RM No 3142, Dec. 1956.

21. Smith, G. A., et al., "Conceptual Study to Apply Advanced Flight Control Technology to the COIN or TRIM Aircraft," Honeywell Inc., 12225-FR(R), AD730571, Jun. 1971.

22. Park, W. J., and Cimbala, J. M., "The Effect of Jet Injection Geometry on Two-Dimensional Momentumless Wakes," J. Fluid Mechanics, Vol. 224, 1991, pp. 29-47.

23. Abramson, J., and Rogers E. O., "High Speed Characteristics of Circulation Control Airfoils," AIAA Paper 83-0265, Jan. 1983.

24. Howe, M. S., "Analytical Study of the Noise Generated by a Coanda Wall Jet Circulation Control Device," Boston University, AM-00-004, Oct. 2000.

25. Louie, L., Fry, D., and Jessup, S., "An Active Control System to Cancel Unsteady Foil Forces," Active Control of Vibration and Noise, ASME, DE-Vol. 75, Nov. 1994.

26. Ham, N.D., Bauer P.H., and Lawrence, T. L., "Wind Tunnel Generation of Sinusoidal Lateral and Longitudinal Gusts by Circulation of Twin Parallel Airfoils," MIT ASRL-TR-174-3, NASA-CR-137547, Aug. 1974.

27. Morgan, W.B., Silovic, V., and Denny, S.B., "Propeller Lifting-Surface Corrections," SNAME Annual Meeting, Nov 1968.